REVISTA DE LA SOCIEDAD GEOLÓGICA DE ESPAÑA

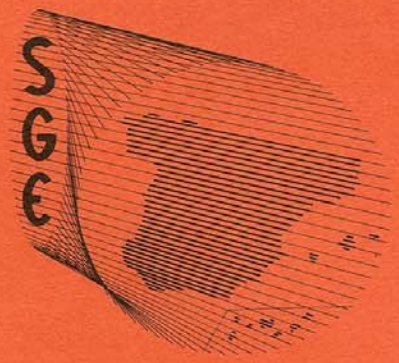

Vol. 4 (1-2) - 1991

LITHOSTRATIGRAPHY, MICROFACIES, AND DEPOSITIONAL ENVIRONMENTS OF THE MESOZOIC OF SIERRA LA NIEVE, COAHUILA, NORTHEAST MEXICO

J.F.Longoria (1) and R.Monreal (2)

(1) Programs in Geosciences, University of Texas at Dallas, Richardson, TX. 75083-0688, ESTADOS UNIDOS.
(2) Escuela Superior de Geociencias, Centro de Estudios Superiores del Estado de Sonora, Hermosillo, Sonora, MEXICO.

ABSTRACT

The stratigraphic succession exposed in the southern limb of La Nieve Anticline is 1600 m thick of predominantly marine carbonate rocks. Six distinctive lithic units (Units I through VI) were recognized based on physical features. This succession was lithocorrelated with units formally established in the region as follows, from bottom to top: Unit I = unknown correlation, Unit II = Cupido Limestone, Unit III = La Peña Formation, Unit IV = likely Tanaulipas Limestone, Unit V = Cuesta del Cura Formation, Unit VI = Agua Nueva Formation. The lower 337 meters of the succession, corresponding to Unit I, are made of siliciclastic sediments, whereas the other 1263 meters, including Units II through VI, are predominantly made of carbonates with minor terrigenous clays and marls. Microfacies analysis of the limestone packages reveled that depositional environments varied from inner ramp to basinal with several regressive-transgressive cycles during the deposition of Unit II. Several biochronologic datum planes were identified: 1) *Favusella* first appearance datum at Sample AR67-3; 2) *Colomiella* first appearance datum at Sample AR68, 3) *Thalmanninella* first appearance datum at Sample AR96-12. Unit II contains miliolid and textularid foraminifera lacking biochronological significance. The Cretaceous succession evolved from a fan-delta environment to a carbonate ramp in an open marine environment during the Lower Aptian (deposition of Unit I) which underwent rapid subsidence accompanied by a major transgressive episode at the beginning of the Albian. Deep marine carbonate depositional environments prevailed from Upper Albian through the Lower Turonian at which time they were replaced by pelitic flysch deposition.

Key words: Mesozoic, stratigraphy, Mexico, global physical events, microfacies, depositional environments.

RESUMEN

La sucesión estratigráfica expuesta en el flanco sur del Anticlinal La Nieve (Coahuila, Norte de México) tiene un espesor de 1600 metros y está constituida por rocas sedimentarias marinas, predominando los carbonatos. Esta sucesión estratigráfica ha sido subdividida en seis unidades líticas (Unidades I a VI) en base a sus características físicas, las cuáles han sido correlacionadas litológicamente con unidades formales previamente descritas en la región. Desde la base al techo son: Unidad I = de difícil atribución, Unidad II = Caliza Cupido, Unidad III = Formación La Peña, Unidad IV = probablemente Caliza Tamaulipas, Unidad V = Caliza Cuesta del Cura, Unidad VI = Formación Agua Nueva. Los 337 metros inferiores de la sucesión estratigráfica, correspondientes a la Unidad I, están constituidos por sedimentos siliciclásticos, mientras que los otros 1263 metros, que incluyen las Unidades II a VI, están compuestos predominantemente por carbonatos con algunas intercalaciones de arcilla y margas terrígenas. El análisis de las microfacies revela que los ambientes sedimentarios variaron desde la rampa interna hasta la cuenca, con varios ciclos regresivo-transgresivos registrados en la Unidad II. Los siguientes biohorizontes fueron identificados: 1) *Favusella* FAD; 2) *Colomiella* FAD; 3) *Thalmanninella* FAD. La historia evolutiva de la sucesión cretácica de la Sierra La Nieve se inició con depósitos de abanico deltáico (depósito de la Unidad I) y pasó a un ambiente de rampa carbonatada de mar abierto en el Aptiense inferior. Esta rampa carbonatada sufrió una rápida subsidencia la cual fue acompañada de un episodio transgresivo mayor al inicio del Aptiense superior. Los depósitos de carbonatos marinos de aguas profundas prevalecieron desde el Albiense superior hasta el Turoniense inferior, momento a partir del cual fueron reemplazados por depósitos del flysch pelítico. Los eventos físicos observados en la sucesión de la Sierra La Nieve son un reflejo de eventos tectóno-eustáticos globales: El evento 1, datado en la base de la biozona *Globigerinelloides maridalensis/Leupoldina cabri* (K-7), coincide con el inicio del ciclo LZB-4.1 de tercer orden; el evento 2, biocronológicamente en la base de la biozona *Ticinella bejaouaensis/Ticinella primula* (K-13), corresponde con la máxima transgresión del ciclo LZB4.2 de tercer orden y marca la inundación (*drowing*) de la rampa

carbonatada; el comienzo de los depósitos de facies flysch, biocronológicamente en la biozona *Thalmanninella appenninica/Rotalipora montasalvensis* (K-17), marca el inicio de la máxima inflexión eustática del Cretácico.

Palabras clave: Mesozoico, Estratigrafía, México, eventos sedimentarios globales, microfacies, ambientes deposicionales.

Longoria,J. and Monreal,R. (1991): Lithostratigraphy, Microfacies and Depositional environments of the Mesozoic of Sierra La Nieve, Coahuila, Northeast Mexico. *Rev. Soc. Geol. España*, 4: 7-31.

Longoria,J. y Monreal,R. (1991): Litoestratigrafía, microfacies y medios sedimentarios del Mesozoico de la Sierra La Nieve, Coahuila, Noreste de México. *Rev. Soc. Geol. España*, 4: 7-31.

1. INTRODUCTION

The Mexican Cordillera contains the most complete marine Mesozoic successions exposed inland in North America. Excellent exposures of continuous Triassic through Cretaceous continental and marine successions can be studied along deeply incised canyons and breached anticlines. Pioneering stratigraphic work in the Sierra Madre Oriental by Bose (1923), Burckhardt (1930), and Imlay (1936, 1937) provided the foundation for modern stratigraphic investigations.

Although the basic concept of microfacies analysis was introduced in the geological literature almost half of century ago by Brown (1943), and it has been successfully used as an integrative tool in sedimentary geology (Cuviller, 1961; Ramírez del Pozo, 1971; Wilson, 1975; Flügel, 1982; Carozzi, 1989), microfacies analysis has received limited application among American geologists. Microfacies analysis (*Ala* Flugel, 1982, and Carozzi, 1989) has the advantage over traditional sedimentological approaches of being interdisciplinary, integrating micropaleontological, stratigraphic, sedimentological, and petrographic aspects to produce paleoecological reconstructions and conceptual depositional models. In few words, microfacies analysis is a dynamic approach to sedimentary geology in which both field and laboratory studies are equally stressed. The present report aims to apply a microfacies approach to the Mesozoic stratigraphic succession exposed at La Nieve Anticline, east of Saltillo, Coahuila (Fig. 1), and to establish its depositional history.

2. REGIONAL GEOLOGICAL SETTING

Sierra La Nieve is located on the eastern edge of the Monterrey Salient of the Sierra Madre Oriental of the Mexican Cordillera (Fig. 1). It is one of the many kilometric scale structures that make the Transverse Range province of the Sierra Madre Oriental between the cities of Monterrey and Torreon and was referred to as Anticlinal Chorro of the Arteaga Anticlinorium by Cserna (1956). The present day geographic position of La Nieve Anticline makes it an ideal target for comparative stratigraphic studies as its depositional setting may help in linking the relatively well-known Jurassic-Cretaceous succession of the Parras area to the west, with that of the Monterrey area to the east.

Sierra La Nieve is an elongated, slightly concave to the south, 22 km long, 2 to 4.5 km wide, NE/SW (N80) trending, doubly plunging, parallel anticlinal fold; twisted along its axial plane (Figs. 1, 2). It varies from symmetric to asymmetric, verging to the N-NE at its northern end, and to the S-SW at its southern end, describing a torsion along its axial surface. La Nieve Anticline reaches a maximum elevation of 3340 meters above sea level and marks the opposite vergence with relation to the frontal ranges of the Sierra Madre Oriental fold belt (Fig. 2). Its southern end is slightly breached and corresponds to "Cañón de El Chorro" through which run Arroyo La Boca and International Highway 57. Cañón de El Chorro is roughly perpendicular to the main structural trend, giving an excellent exposure of the entire stratigraphic succession (Fig. 1).

2.1. Previous Investigations

Previous work on El Chorro succession has been concentrated on detailed sedimentological and petrographic studies of some parts of the section: A study of the diagenesis of the Cupido Formation in El Chorro Canyon was done by Guzmán (1974). Ekdale *et al.* (1976) presented a numerical analysis of carbonate microfacies of the Cupido Limestone. Wilson and Pialli (1977) included Los Chorros section in their regional correlation of Lower Cretaceous strata of northeastern Mexico. Wilson (1981) studied the cyclicity in the Cupido carbonates. Salisbury (1982) studied the petrology and diagenesis of "La Casita Formation". Fortunato (1982) and Fortunato and Ward (1982) studied the depositional systems of "La Casita Formation". Recently, paleomagnetic studies of the "Aurora Limestone" and the Cupido Formation were undertaken by Bonfiglio (1982) and Kliest *et al.* (1984), respectively.

3. STRATIGRAPHY

3.1. The problem

Very little effort has been given to systematically

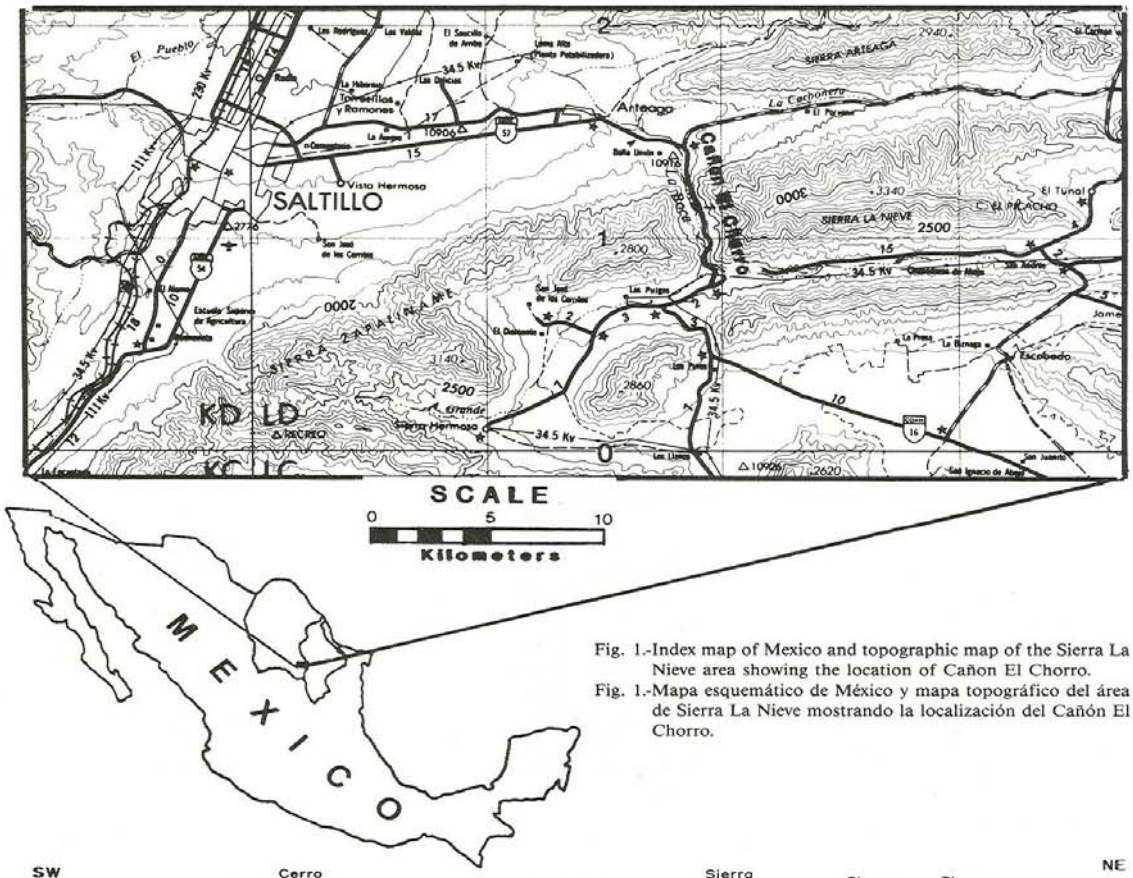

Fig. 1.-Index map of Mexico and topographic map of the Sierra La Nieve area showing the location of Cañon El Chorro.

Fig. 1.-Mapa esquemático de México y mapa topográfico del área de Sierra La Nieve mostrando la localización del Cañón El Chorro.

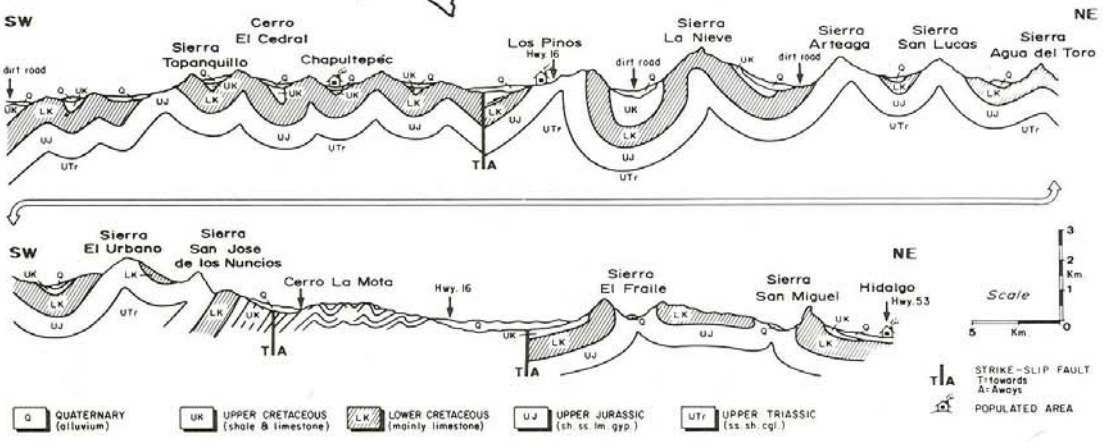

Fig 2.-Regional NE-SW structural section across the Transverse Ranges of the Sierra Madre Oriental, states of Nuevo Leon and Coahuila, Mexico showing the position and geometry of Sierra de La Nieve anticline. Note the SW vergence of Sierra La Nieve corresponding to its southern end, opposite to the NE vergence of the frontal range Sierra San José de los Nuncios.

Fig. 2.-Perfil estructural regional, NE-SW, del Sector Transverso de la Sierra Madre Oriental, estados de Nuevo León y Coahuila, México, mostrando la posición y geometría del anticlinal Sierra La Nieve. Nótese la vergencia hacia el SW de este anticlinal, que es opuesta a la NE del anticlinal frontal de la Sierra de San José de los Nuncios.

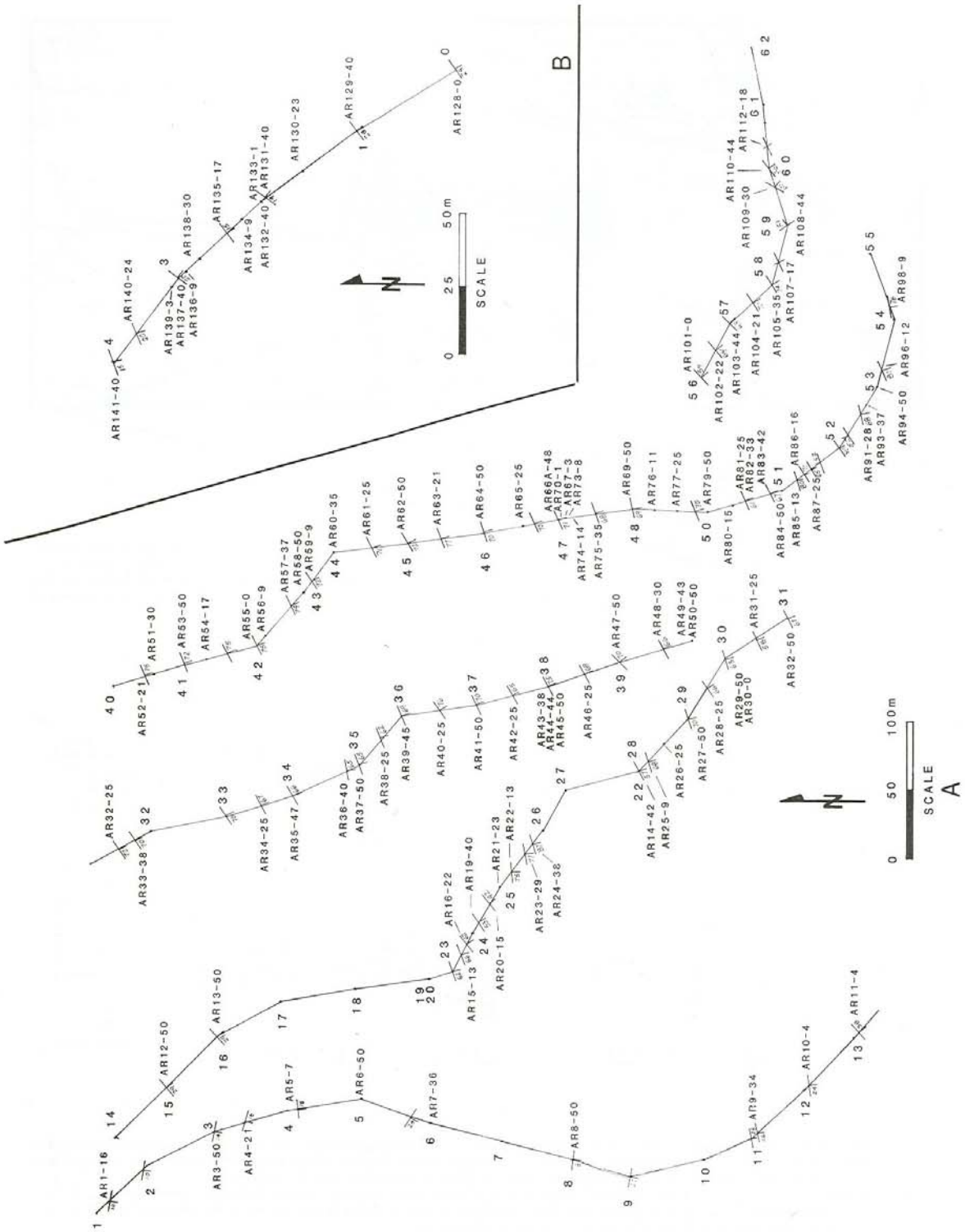
B
N
SCALE
0 25 50m
A
N
SCALE
0 50 100m

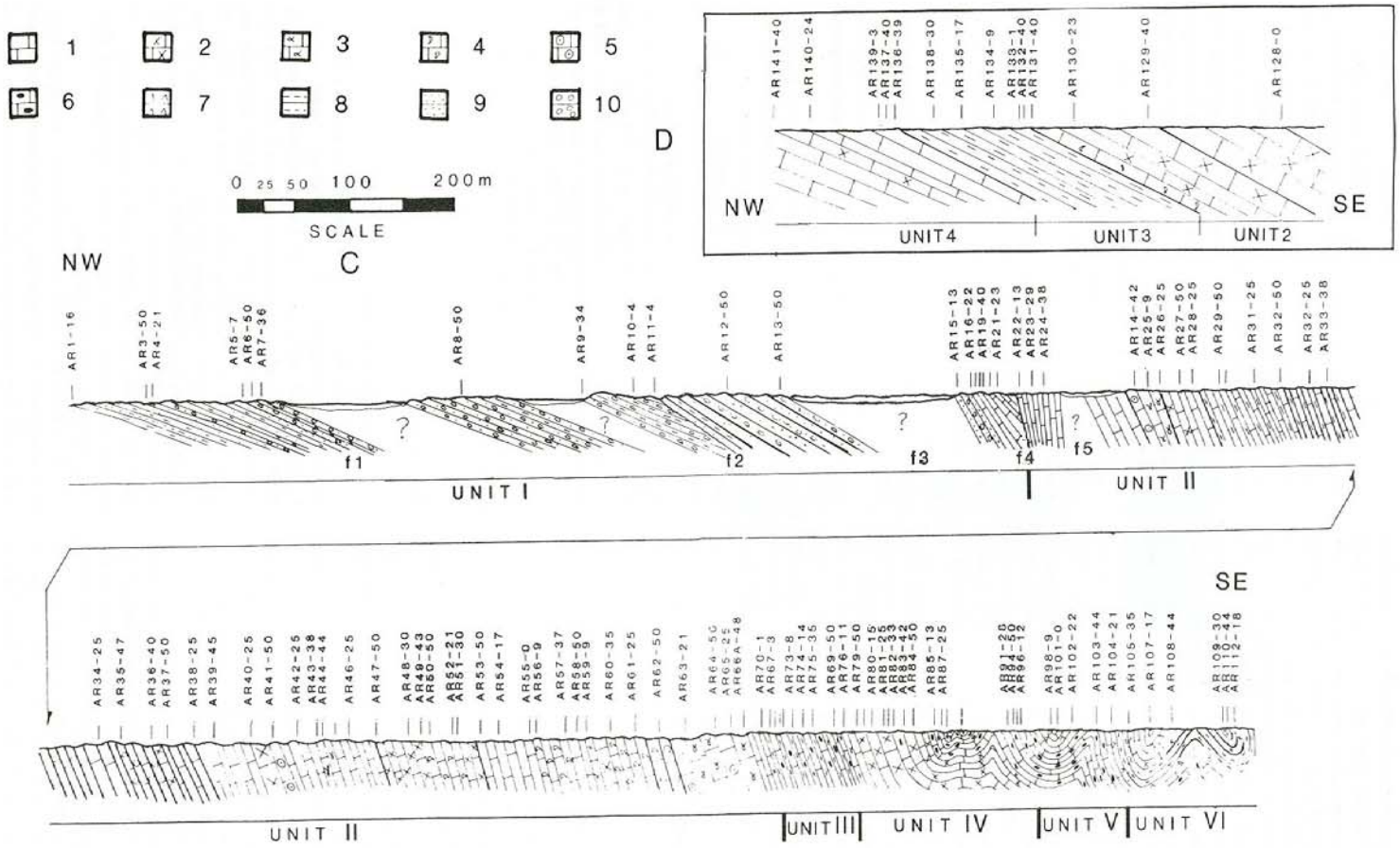

Fig. 3.-Field data showing the attitude of strata along the Mesozoic succession exposed along Cañon El Chorro. A: Plan view of field traverse along Highway 57 through Cañon El Chorro, showing bearing stations, structural attitude of lithic units, and sample locations. B: Plan view of La Peña Formation outcrop exposed along between kilometer marks 39 and 40 of Highway 57. C: Structural cross section across the southern limb of Sierra La Nieve Anticline as observed along Highway 57, showing lithic packages recognized (Units I through VI) and the nature of their contacts. D: Cross section of La Peña Formation outcrop along traverse shown in fig. 3B. Note reverse stratigraphic succession of this locality.

Fig. 3.-Datos de campo mostrando la posición de los estratos a lo largo de la sucesión Mesozoica expuesta en el Cañón El Chorro. A: Vista en planta de la travesía sobre la Carretera 57, a lo largo del Cañon El Chorro, mostrando las estaciones, posición estructural y localización de las muestras. B: Vista en planta del afloramiento de la Formación La Peña expuesto en los kilometros 39 y 40 de la Carretera 57. C: Reconstrucción estructural del flanco Sur del anticlinal La Nieve tal como se observa sobre la Carretera 57, mostrando las unidades líticas reconocidas en el presente estudio así como la naturaleza de sus contactos. D: Reconstrucción estructural del afloramiento de la Formación La Peña mostrado en al figura 3B. Nótese la inversión estratigráfica del afloramiento.

study the lithostratigraphy of the Mesozoic of northern Mexico beyond the original work by pioneer geologists, making recent paleogeographic reconstructions of Mexico highly speculative (Longoria, 1988). Consequently, a constant misidentification of lithic units is found in the literature, to the extreme that even formations such as La Caja, La Casita, Cupido, La Peña, and Aurora can not be used as paleogeographic indicators. Amazingly, in spite of their constant use in recent geologic studies, there is not published record of any attempt to study the type localities of the aforementioned formations after their original introduction in the geological literature at the beginning of this century. A full discussion on the many examples of the misuse of lithostratigraphic concepts is outside the scope of this paper. Some of these problems, however, have been addressed elsewhere (Longoria, 1984a,b; 1988). Nonetheless, it is evident that a systematic stratigraphic method is needed to obtain paleoenvironmental data meaningful in paleogeographic reconstructions.

It is a common practice to assign a chronostratigraphic position to an outcrop based on its assumed lithostratigraphic designation, thus the assumption of isochronous lithic units is deeply entrenched in the literature. Furthermore, very little is known on the depositional environments and microfacies characterization of the Mesozoic lithostratigraphic units of northeastern Mexico beyond their broad paleogeographic setting.

3.2. *Lithostratigraphic succession of Sierra La Nieve*

3.2.1. *Methods*

The stratigraphic succession of the south limb of La Nieve Anticline exposed along highway 57 was studied according to the following procedures:

a.- The succession was separated into lithic packages based on physical properties as observed in the field, including bedding thickness, lithic types, and geomorphic expression. Although we consider the Formation to be the basic unit in lithostratigraphy, we also believe that the first step in lithostratigraphic work should be an objective inventory of lithic packages as exposed in the area under study, instead of an a-priori adoption of nomenclatural terms (formation names), that may not relate to the exposed succession. Thus, no formational names were used at this stage to avoid subjective biases in the inventory of the lithic features and establishment of lithic units. Units recognized during this part of the study were numbered, from base to top, using roman numerals.

b.- The entire succession was measured using the tape and Brunton method. Samples were taken at intervals varying from 5 to 25 meters. A plan view of the traverse was plotted at the scale of 1: 25,000, and true thickness of the units were obtained using a graphic method (Fig. 3A). A cross-section of the plan view of the traverse was obtained (Fig. 3B) which depicted the nature of the formational contacts and the structural style of each unit.

c.- Lithocorrelation of our lithic packages, units established by us in Step 1 as above, with formally established units was undertaken. Both direct, i.e. field comparisons with the type localities of Jurassic and Cretaceous formations in the region, and indirect, i.e. via literature, lithocorrelations were undertaken. Unfortunately, as it is discussed below, three of the lithic units exposed in El Chorro Canyon could not be assigned with certainty to the units they have been referred to by previous workers.

d.- Microfacies analysis *Ala* Flugel (1982), *i.e.*, identification of all paleontological and petrographic components of the rock as observed in thin-section was undertaken.

e.- Planktonic foraminifera, nannoconid and calpionellid taxa were identified in thin-section using the taxonomic criteria defined by Bonet (1956), Pessagno (1967), Longoria (1968, 1975), and Longoria and Gamper (1974). Later, these taxa were referred to the biochronologic scheme established by Longoria (1984c) for Mexico and the Gulf Coastal Plain.

f.- An interpretation of depositional systems and depositional environments using physical satratrigraphy and microfacies data was finally made.

The stratigraphic succession exposed on the south limb of La Nieve Anticline is about 1600 meters thick (Figs. 3, 4). The lower 337 meters are made of terrigenous sediments while the rest is composed mostly of carbonates with only minor shale intervals.

During the present investigation field work was carried out with the purpose of establishing lithic packages based on physical features such as 1) lithologic types, 2) types of stratification, 3) bedding thickness, and 4) geomorphic expression of packages. This inventory resulted in the establishment of six lithic packages within the succession exposed at La Nieve Anticline (Figs. 3 and 4). These units are described below, from bottom to top.

3.3. *Unit I*

3.3.1. *Description*

Irregular alternation of sandstone, manily arkosic, shale and conglomerate; individual beds varying frommedium- to massive- bedded; parallel, even stratification throughout; weathers yellowish-tan. This unit is exposed between stations 1 and 25 of our field traverse (Fig. 3A), including samples AR1-16 to AR21-23 (Fig. 4). A total thickness of about 367 meters is exposed. Shales are more abundant in the lower part, and become locally carbonaceous. Conglomerates become more abundant in the upper part and range from fine- to coarse-grained. The upper 30 m. are made of thin- to medium-bedded limestone.

The base of Unit I is not exposed, the upper contact is marked by an angular unconformity and is placed at the first occurrence of homogeneously bedded limestone of Unit II (Figs. 3 and 4; sample AR22-13).

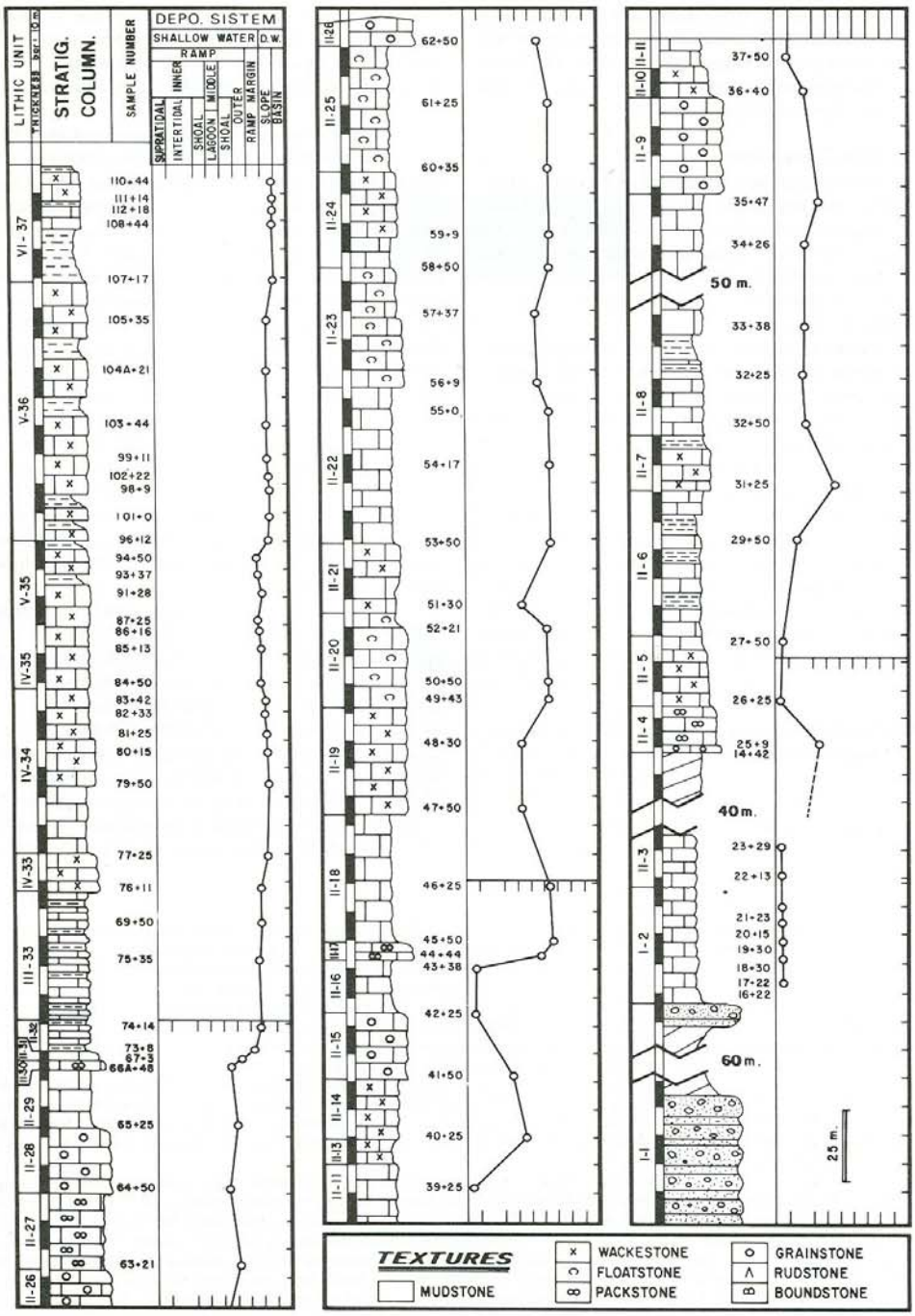

Fig. 4.-Columnar representation of the Mesozoic succession depicting lithic units (roman numerals), microfacies (arabic numerals) and the evolution of depositional systems. The chronostratigraphic position of the units is discussed in the text.

Fig. 4.-Representación en columnas estratigráficas del Mesozoico, mostrando las unidades líticas (números romanos), microfacies (números arábigos) y la evolución de los sistemas deposicionales. La posición cronoestratigráfica de las unidades se discute en el texto.

In the middle part of this unit, at station 13 of the field traverse, sample AR11-4, a disconformity and an angular unconformity were observed (Fig. 3B). Three covered intervals between stations 6 and 8, 9 and 11, and 16 and 23 are present (Figs. 3 and 4).

3.3.2. Lithocorrelation

Unit I was referred to La Casita Formation by Fortunato (1982) and Fortunato and Ward (1982). However, our comparative studies with the type La Casita indicate that Unit I is not assignable to the former unit because it does not display the limestone and shale alternations rich in phosphatic nodules which characterize La Casita stratotype.

Unit I displays similar features to La Gloria Formation of Imlay (1936) as exposed in Cañon Taraises of Sierra de Parras, Coahuila. According to Imlay (1936) at its type locality, La Gloria is predominantly made of terrigenous sand and conglomerate with only a few thick-bedded limestone layers. These limestone layers are found at the top and bottom of the La Gloria stratotype. Later, Imlay (1937, p. 599) referred to La Gloria a lithic succession predominantly made of thick- to medium-bedded gray limestone exposed on the north wall of Cañón Mimbre. The present authors were unable to locate Imlay's La Gloria outcrop in Cañon Taraises; however, at Cañón del Mimbre we found a think succession made of dark-gray to black, evenly bedded limestone and minor shale interbeds which indeed correspond to Imlay's (1937) concept of La Gloria.

Similar lithic packages to Unit I and Imlay's outcrop from Cañón Taraises were described by Burckhardt (1930) from several localities in northern Mexico and assigned to the Lower Cretaceous. In any case, the lithic features displayed by Unit I are more related to 'La Gloria' sensu Imlay (1936) than to La Casita. Nonetheless, in the present investigation Unit I is not lithocorrelated with certainty to neither La Gloria nor La Casita. Further comparative lithostratigraphic studies are needed to define the nature of La Gloria.

3.3.3. Fossils and Chronostratigraphic Position

Lower Aptian (Bedoulian, Biozone K-6). No fossils were found in the samples collected from Unit I during the present investigation. The present chronostratigraphic designation is based on the concurrence range of the fossils reported from this unit. The type La Gloria was doubtfully assigned to the Oxfordian by Imlay (1936, p. 1109) based on his assumed correlation with the *Nerinea*-bearing limestones described by Burckhardt (1930) from northern Zacatecas and southeastern Durango. Similarly, "La Gloria" sensu Imlay (1936), can be assigned to the Lower Cretaceous based on its resemblance to unnamed Lower Cretaceous units described by Burckhardt (1930) from the same areas in northeastern Mexico. However, there is no faunal evidence to document Imlay's original Oxfordian assignation to the La Gloria. Furthermore, it is likely that other lithologically similar Lower Cretaceous units also described by Burckhardt (1930) may have been lumped in "La Gloria'.

Other authors (Fortunato, 1982, Fortunato and Ward, 1982, Wilson and Pialli, 1977, Barrier, 1977) reported nannofossils from Unit I, 230 meters below the Cupido contact, among them are *Nannoconus steinmanni* Kampter, *N. globulus* Bronnimann, *Cruciellipsis chiasta* (Wrsley), and *Parhabdolitus asper* (Stradner). This assemblages is indicative of the Bedoulian. *Parhabdolitus asper* (Stradner) is common in the Bedoulian-Albian stratotypes of France (Manivit, 1971, p. 86). On the other hand, *Cruciellipsis chiasta* (Wrsley) was reported from the Lower Berriasian-Cenomanian

Fig. 5.-Microfacies characteristics and grain types observed in Unit II: 1) Biomicrite. Echinoderm spine, and mollusk fragments. Sample AR23-39. Unit II-3. 2) Fossiliferous micrite. Pelecypod fragments. Sample AR22-13, Unit II-3. 3) Fossiliferous micrite. Echinoderm fragment, dolomite-crystals. Cross nichols. Sample AR27-50. Unit II-5. 4) Biomicrite. Rudist shell fragment. Sample AR26-25. Unit Unit II-5. 5) Biomicrite. Miliolids. Sample AR31-25. Unit II-7. 6) Biomicrite. Miliolid ?. Sample AR31-25. Unit II-7. 7) Microsparite-pseudosparite. Sample AR34-25. Unit II-8. 8) Biomicrite. Intraclast. Sample AR31-25. Unit II-7. 9) Fossiliferous micrite. Miliolid. Sample AR32-50. Unit II-8. 10) Fossiliferous micrite. Nummoloculina sp. Sample AR42-25. Unit II-8. 11) Biomicrite. Pelecypod shell fragments. Sample AR33-38. Unit II-5. 12) Fossiliferous micrite. Pelecypod shell fragments. Sample AR20-15. Unit I-2. 13) Biomicrite. Mollusk fragment with advanced neomorphism. Sample AR26-25. Unit II-5. 14) Sample AR31-25. Biomicrite. Unit II-7. Pelecypod shell fragments. 15) Sample AR35-47. Biopelsparite. Unit II-9. Leached allochems, micritic envelopes. 16) Sample AR35-47. Biopelsparite. Unit II-9. Leached allochem, micritic envelopes, authigenic quartz. 17) Sample AR25-9. Packed biomicrite. Unit II-4. Ostracods, pellets. 18) Sample AR39-45. Biointrasparite. Unit II-12. Gastropod, micritic envelopes. 19) Sample AR39-45. Biointrasparite. Unit II-12. Mollusk shell fragment, micritic envelopes. 20) Sample AR25-9. Packed biomicrite. Unit II-4. Green algae ?. Scale bar = 200 microns for all figures.

Fig. 5.-Tipos de granos y microfacies características identificados en la Unidad II: 1) Biomicrita. Espina de equinodermos y fragmentos de molusco. Muestra AR23-39. Unidad II-3. 2) Micrita fosilífera. Fragmentos de pelecípodo. Muestra AR22-13, Unidad II-3. 3) Micrita fosilífera. Fragmento de equinodermo, cristales de dolomita (Luz polarizada). Muestra AR27-50. Unidad II-5. 4) Biomicrita. Fragmento de rudista. Muestra AR26-25. Unidad II-5. 5) Biomicrita. Miliólidos. Muestra AR31-25. Unidad II-7. 6) Biomicrita. (¿Miliólido?. Muestra AR31-25. Unidad II-7. 7) Microesparita-pseudoesparita. Muestra AR34-25. Unidad II-8. 8) Biomicrita. Intraclasto. Muestra AR31-25. Unidad II-7. 9) Micrita fosilífera. Miliólido. Muestra AR32-50. Unidad II-8. 10) Micrita fosilífera. *Nummoloculina* sp. Muestra AR42-25. Unidad II-8. 11) Biomicrita. Fragmentos de pelecípodo. Muestra AR33-38. Unidad II-5. 12) Micrita fosilífera. Fragmentos de pelecípodo. Muestra AR20-15. Unidad I-2. 13) Biomicrita. Fragmento de molusco con neomorfismo avanzado. Muestra AR26-25. Unidad II-5. 14) Muestra AR31-25. Biomicrita. Unidad II-7. Fragmentos de pelecípodo. 15) Muestra AR35-47. Biopelesparita. Unidad II-9. Aloquímicos con envueltas micríticas. 16) Muestra AR35-47. Biopelesparita. Unidad II-9. Alloquímico disuelto con envoltura micrítica, cuarzo autigénico. 17) Muestra AR25-9. Biomicrita empaquetada. Unidad II-4. Ostrácodos. 18) Muestra AR39-45. Biointraesparita. Unidad II-12. Gasterópodo, con recubrimientos micríticos. 19) Muestra AR39-45. Biointraesparita. Unidad II-12. Fragmento de molusco con envoltura micrítica. 20) Muestra AR25-9. Biomicrita. Unidad II-4. ¿Algas verdes?. Escala = 200 micras para todas las figuras.

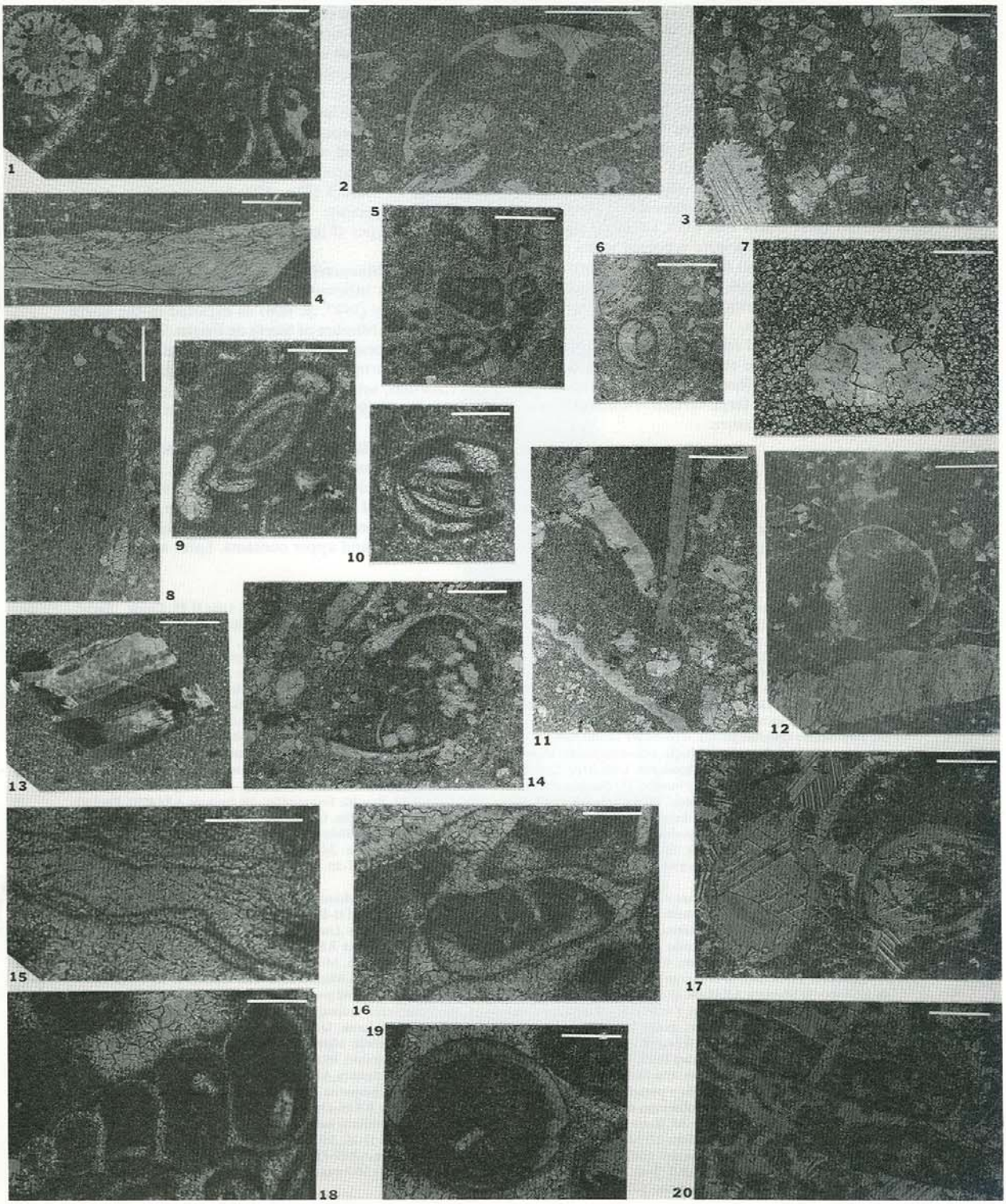
1
2
3
4
5
6
7
8
9
10
11
12
13
14
15
16
17
18
19
20

of France (Thierstein 1972, p. 41). Furthermore, *Nannoconus steinmanni* Kampter, *N. globulus* Bronnimann are found in the pelagic facies of Mexico from the base of Biozone K-1 though the top of Biozone K-6 *(Globigernielloides gottisi/Globigerinelloides maridalensis* Interval-Zone of the zonal scheme by Longoria (1984c).

Additionally, Fortunato and Ward (1982, p. 475) reported the occurrence of Hauterivian-Valanginian ammonites in the upper part of Unit I which further complicates the issue. According to them (op. cit. p. 475) the alleged fossils occur 366 meters above the base of their section (just below our Unit I-Unit II contact).

Benthic foraminifera were reported to be present in this unit by Fortunato (1982, p. 27), unfortunately none of the benthic species listed by her have restricted chronostratigraphic distribution and range from Jurassic to Lower Cretaceous.

The fossils reported from Unit I by the aforementioned authors are herein regarded as re-worked Lower Cretaceous (Berriasian-Barremian) into the Lower Aptian, which explains the large variation in fossil assemblages as well as its mixture.

3.4. Unit II

3.4.1. Description

Homogeneous package of limestone (mudstone to grainstone) varying from thick- to massive-bedded; parallel, even stratification throughout; weathers gray to light-gray. This unit is exposed between stations 25 and 47, including samples AR22-13 to AR70-1 (Figs. 3, 4) of our field traverse. A total thickness of about 934 meters is exposed, the lower contact with Unit I is marked by an angular unconformity. The upper contact with Unit 3 is sharp and was placed at the base of the first stratigraphic occurrence of thin- to medium-bedded limestone of Unit 3 (Fig. 3B). In spite of its megascopic homogeneity, Unit II contains 29 different microfacies types (Figs. 4A-D).

3.4.2. Lithocorrelation

Unit II is lithocorrelated with the Cupido Limestone of Imlay (1937, p. 606) as exposed in the north wall of Cañón Mimbre of Sierra de Parras. The La Nieve limestone succession closely resembles a section exposed in the nearby Sierra de los Muertos in Cañón de Las Cabrillas, southeast of the town of Higueras, which Humphrey (1949, p. 102) also referred to as Cupido.

3.4.3. Fossils and Chronostratigraphic Position

Aptian (Biozone K-7 to Biozone K-12). Imlay (1936, p. 607) doubtfully assigned the Cupido to the upper Hauterivian and Barremian, based on the chronostratigraphic position of the adjoining units, assuming conformable lower and upper contacts. Later authors have

Fig. 6.-Microfacies characteristics and grain types observed in Units II and III: 1) Sample AR41+50. Biosparite. Unit II-15. Ooids. 'Early' and 'late' cements. 2) Sample AR49-43. Biopelmicrudite. Unit II-20. Green algae?. 3) Sample AR48-50. Biomicrite. Unit II-19. Mollusk fragment. 4) Sample AR44-44. Biointrasparite. Unit II-17. Leached allochems, echinoderm fragment, micritic envelopes. 'Early and 'late' cements. 5) Sample AR48-30. Biomicrite. Unit II-19. Unidentified benthic foraminifer. 6) Sample AR42-25. Fossiliferous micrite. Unit II-16. Miliolid. 7) Sample AR41-50. Biosparite. Unit II-15. Ooids, two generations of cement are seen. 8) Sample AR42-25. Fossiliferous micrite. Unit II-16. Mollusk shell fragment. 9) Sample AR44-44. Packed biointrasparite. Unit II-17. Reworked grapestone. 10) Sample AR62-50. Packed biopelsparite. Unit II-26. Peloids and miliolid. 11) Sample AR44-44. Packed biointramicrite. Unit II-17. Leached allochems, micritic envelopes, unidentified grain. 12) Sample AR70-1. Biomicrite. Unit III-32. Unidentified planktonic foraminifer (Hedbergella?). Coalescive neomorphism. 13) Sample AR47-50. Biomicrite. Unit II-19. Milliolid. Microsparite and pseudosparite. 14) Sample AR41-50. Biointrasparite. Unit II-15. Packed ooids with miliolid nuclei, intraclast. Two generations of cement. 15) Sample AR48-30. Biomicrite. Unit II-19. Quinqueloculinid miliolid. 16) Sample AR47-50. Biomicrite. Unit II-19. Radial ooid, microspar and pseudospar matrix. 17) Sample AR44-44. Packed biointrasparite. Unit II-17. Radial ooid with miliolid nuclei. Two generations of cement are seen. 18) Sample AR49-43. Biomicrite. Unit II-19. Benthic foraminifer. 19) Sample AR64-50. Packed biopelmicrite. Unit II-28. Pellets, benthic foraminifera. 20) Sample AR39-45. Biointrasparite. Unit II-12. Miliolid. 21) Sample AR62-50. Biopelsparite. Unit II-26. Quinqueloculinid miliolids, pellets. 22) Sample AR56-9. Fossiliferous micrite. Unit II-22. Pelecypod shell fragments. 23) Sample AR49-43. Biopelmicrudite. Unit II-20. Mollusk shell fragments. 24) Sample AR35-47. Biopelsparite. Unit II-9. Ooids?. Coalescive neomorphism. 25) Sample AR49-43. Biopelmicrudite. Unit II-20. Miliolid. Scale bar = 200 microns for all figures.

Fig. 6.-Tipos de granos y microfacies características identificados en las Unidades II y III: 1) Muestra AR41-50. Bioesparita. Unidad II-15. ooides. Cementos 'temprano' y 'tardio'. 2) Muestra AR49-43. Biopelmicrorrudita. Unidad II-20. (¿Algas verdes?. 3) Muestra AR48-50. Biomicrita. Unidad II-19. Fragmento de molusco. 4) Muestra AR44-44. Biointraesparita. Unidad II-17. Aloquímicos disueltos, fragmento de equinodermo y envolturas micríticas. Cementos temprano y tardío. 5) Muestra AR48-30. Biomicrita. Unidad II-19. Foraminífero bentónico indeterminado. 6) Muestra AR42-25. Micrita fosilífera. Unidad II-16. Miliólido. 7) Muestra AR41-50. Bioesparita. Unidad II-15, ooides, se observan dos generaciones de cemento. 8) Muestra AR42-25. Micrita fosilífera. Unidad II-16. Fragmento de molusco. 9) Muestra AR44-44. Biointraesparita empaquetada. Unidad II-17. *Reworked grapestone.* 10) Muestra AR62-50. Biopelesparita. Unidad II-26. Peloides y miliólidos. 11) Muestra AR44-44. Biointramicrita empaquetada. Unidad II-17. Aloquímicos disueltos, con envolturas micríticas, grano indeterminado. 12) Muestra AR70-1. Biomicrita. Unidad III-32. Foraminífero planctónico indeterminado (Hedbergella?). 13) Muestra AR47-50. Biomicrita. Unidad II-19. Miliólido. Microesparita y pseudoesparita. 14) Muestra AR41-50. Biointraesparita. Unidad II-15. Ooides empaquetados con núcleo de miliólido, intraclasto. Dos generaciones de cemento. 15) Muestra AR48-30. Biomicrita. Unidad II-19. Miliólido (quinqueloculina). 16) Muestra AR47-50. Biomicrita. Unidad II-19. Ooide radial, matriz de microesparita y pseudoesparita. 17) Muestra AR44-44. Biointraesparita empaquetada. Unidad II-17. Ooide radial con núcleo de miliólido. Se observan dos generaciones de cemento. 18) Muestra AR49-43. Biomicrita. Unidad II-19. Foraminífero bentónico. 19) Muestra AR64-50. Biopelmicrita. Unidad II-28. Pelloides, foraminíferos bentónicos. 20) Muestra AR39-45. Biointraesparita. Unidad II-12. Miliólido. 21) Muestra AR62-50. Biopelesparita. Unidad II-26. Miliólidos quinqueloculínidos. 22) Muestra AR56-9. Micrita fosilífera. Unidad II-22. Fragmentos de pelecípodo. 23) Muestra AR49-43. Biopelmicrudita. Unidad II-20. Fragmentos de molusco. 24) Muestra AR35-47. Biopelesparita. Unidad II-9. ooides?. 25) Muestra AR49-43. Biopelmicrorrudita. Unidad II-20. Miliólido. Escala = 200 micras para todas las figuras.

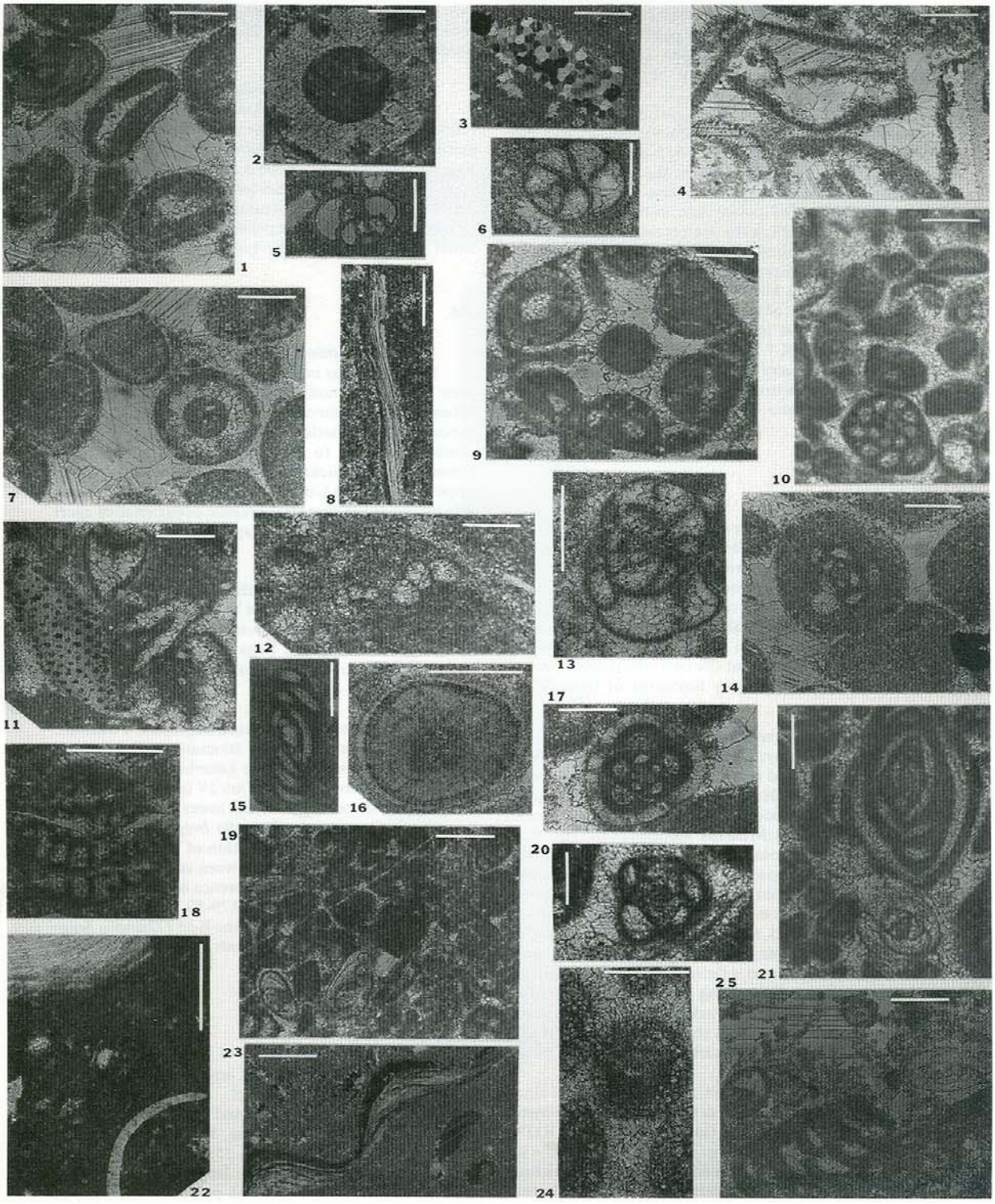
1
2
3
4
5
6
7
8
9
10
11
12
13
14
15
16
17
18
19
20
21
22
23
24
25

assumed a Hauterivian-Barremian chronostratigraphic position of the Cupido without paleontologic evidence. Muslow (1983) reported *Orbitolina, Dictyoconus, Choffatella,* and *Chondrodonta* from the Cupido in San Lorenzo Canyon.

Only benthic microfossils, including the foraminifera *Orbitolina* s.l. (sample AR59-9) and *Nummoloculina* sensu Bonet (1956), (Fig. 5-9, 5-10; Fig. 6-15, 20-21) were observed during the present study. This faunal association defines an Aptian-Albian concurrent range, but the presence of Lower Aptian microfossils in the upper part of Unit I, a few meters below the unconformable contact with the Cupido, and the occurrence of Upper Aptian (Clansayesian, Biozone K-13) at the base of the overlaying Unit III constrain the chronostratigraphic position of the Cupido exposed at El Chorro Canyon from post lowermost Lower Aptian (Bedoulian), Biozone K-7 *(Globigerinelloides maridalensis/Leupoldina cabri* Interval-Zone) to Upper Aptian (Clansayesian), Biozone K-12 *(Ticinella ferreolensis/Ticinella bejaouaensis* Interval-Zone).

3.5. Unit III

3.5.1. Description

Irregular alternation of limestone, shale, marl, and chert; thin-bedded, parallel, even stratification throughout; weathers dark-brown, marls are reddish. Unit III is exposed between stations 47 and 48 of our field traverse (Figs. 3A-B), including samples AR67-3 to AR69-50 (Fig. 4). A total thickness of 55 meters is exposed. The upper contact with Unit IV is sharp but concordant and was placed at the first stratigraphic occurrence of thick-bedded gray limestone of Unit IV.

3.5.2. Lithocorrelation

Unit III displays lithic features such as marly layers and thin-bedded argillaceous limestone that resemble La Peña sensu Humphrey (1949, p. 103-104, plate 2, figure 1), as exposed in Rincón de San Gregorio, north flank of Los Muertos Anticline. On the other hand, this unit is considerably thinner compared with the La Peña as exposed in La Boca Canyon, whereby it displays a threefold division (Longoria and Dávila, 1978); however, it is evident that both successions formed in response to a diastrophic event marking an abrupt lithologic change. In El Chorro section this contact is well exposed and is defined by the superposition of limestone beds containing planktonic foraminifera (above) and miliolid-rich wackestones and grainstones (below). It is also clear that the deposition of this unit marks the interruption of carbonate deposition of the Cupido ramp.

A supplementary section of La Peña exposed along highway 57, a few kilometers south between kilometer posts 39 and 40 was studied (samples AR132 to AR137). At this locality La Peña (Fig. 3A) is exposed on the lower limb of a large overturned to recumbent anticlinal fold. Here the formation consists of a regular alternation of marl and clayey limestone and contains planktonic foraminifera such as *Ticinella* and *Globigerinelloides.*

3.5.3. Fossils and Chronostratigraphic Position

The lowermost part of Unit III (Samples AR67-3; AR68-25) contains abundant planktonic foraminifera among them *Hedbergella delrioensis* (Carsey), *Favusella scitula* Michael, *Favusella confusa* Longoria, and *Ticinella* sp. as well as *Colomiella mexicana* Bonet indicative of the uppermost Aptian Biozone K-13 *(Ticinella bejaouaensis/Ticinella primula* Interval-Zone of the zonal scheme proposed by Longoria, 1984c).

3.6. Unit IV

3.6.1. Description

Homogeneous package of thick-bedded limestone with black chert nodules; parallel, even stratification throughout the interval; weathers light-gray. Unit IV is exposed between stations 48 and 51 (Fig. 3A), including samples AR76-11 to AR84-50 (Figs. 4) of our field traverse. A total thickness of 85 meters is exposed. The upper contact with Unit V is sharp but concordant, and was placed at the first stratigraphic occurrence of chert layers of Unit V. Unit IV displays dekametric folds.

3.6.2. Lithocorrelation

Unit IV can not be precisely assigned to a lithostratigraphic unit; however, it closely resembles the limestone package above La Peña as exposed at La Boca Canyon of Cerro de La Silla (SE of Monterrey) referred to Tamaulipas Limestone by Longoria and Dávila (1978, p. 78-80).

3.6.3. Fossils and Chronostratigraphic Position

Albian, Biozone K-14 to Biozone K-15. The concurrence of *Ticinella primula* Luterbacher and *Colomiella* sp. in the lower part of Unit IV (samples AR69-50 to AR77-25) is indicative of the lower Albian Biozone K-14 *(Ticinella primula/Ticinella breggensis* Interval-Zone). The stratigraphic extinction of members of *Colomiella,* which takes place between samples AR77-25 and AR79-50, as well as the presence of *Ticinella breggensis* (Gandolfi) in sample AR79-50, assigns this horizon to the upper Albian Biozone K-15 *(Ticinella breggiensis/Thalmanninella ticinensis Interval-Zone).*

3.7. Unit V

3.7.1. Description

Homogeneous package of limestone and chert layers; medium-bedded, parallel, wavy stratification; weathers gray. Unit V is exposed between stations 51 and 58 of our field traverse (Fig. 3A), through the waterfall "El Chorrito" (station 55), including samples AR85-13 to AR107-17 (Fig. 4). Its upper contact with Unit VI is transitional and was placed at the base of

the shale, bentonite, and limestone alternations of Unit VI. A total thickness of about 128 meters is exposed.

3.7.2. Lithocorrelation

Unit V is herein assigned to Cuesta del Cura Limestone because it displays the wavy stratification and chert layers that typify the Cuesta del Cura as described by Imlay (1936, p. 1125-1126; 1937, p. 613-615) from the Sierra de Parras. The El Chorro section is also remarkably similar to the lithologies of the same unit exposed at la Boca Canyon of Cerro de La Silla.

3.7.3. Fossils and Chronostratigraphic Position

Vraconian-Cenomanian, Biozone K-16 tp Biozone K-17. The base of Unit V (samples AR85-18 through AR94-50) lacks biochronologic markers. The first stratigraphic occurrence of single-keeled *Hedbergelloidea (Thalmanninella ticinensis* Gandolfi) indicative of Biozone K-16 *(Thalmanninella ticinensis/Thalmanninella appenninica* Interval-Zone) in the Vraconian, takes place in sample AR96-12 (Fig. 4). The first appearance of *Thalmanninella evoluta* (Brotzen) occurs in sample AR103-44 assigning the upper part of Unit V to Biozone K-17 *(Thalmanninella appenninica/Rotalipora monsalvensis* Interval-Zone).

3.8. Unit VI

3.8.1. Description

Irregular alternation of shale, argillaceous limestone and bentonite beds; thin- to medium-bedded; parallel, even stratification; weathers dark-gray to tan. Unit VI is exposed from station 58 trough 61 (Fig. 3A), including samples AR108-44 to AR110-44 of our field traverse (Fig. 3). Only 40 meters of this unit are exposed along Highway 57, but it is well exposed in the valley directly north of "El Chorrito" waterfall where Unit VI is involved in several tight isoclinal folds. Its upper contact is not exposed. At a regional scale, Unit VI forms the synclinal valley that separates La Nieve and Los Pinos anticlines.

3.8.2. Lithocorrelation

Unit VI is herein assigned to the Agua Nueva because it displays the typical alternation of thin-bedded shale, shaley limestone, and bentonite that characterizes this unit at its type locality in the Borrega Canyon of Sierra de Tamaulipas. It was not possible; however, to distinguish the three-fold division of the Agua Nueva as originally viewed by Muir (1936, p. 44). El Chorro section is also closely similar to the succession exposed along La Boca Canyon in Cerro de La Silla as described by Longoria and Dávila (1978, p. 81-82).

3.8.3. Fossils and Chronostratigraphic Position

Cenomanian, Biozone K-17 to Biozone K-18. The lowermost part of Unit VI is referable to Biozone K-17 as it contains *Thalmanninella evoluta* (Sigal). The first occurrence of the foraminiferal genus Rotalipora takes place in sample AR108-44 which delineates the base of Biozone K-18 *(Rotalipora montsalvensis/Rotalipora cushmani* Interval-Zone) of the Lower Cenomanian.

4. MICROFACIES

4.1. Methods

Samples collected were slabbed and thin-sectioned using standard petrographic procedures. Thin-sections were studied for microfacies analysis (Ala Flugel, 1982; and Carozzi, 1989) and a photo-atlas with all the microfacies types was elaborated. Representative examples of these microfacies are illustrated in figures 5, 6, 7, and 8. These figures illustrate the microfaunal content of the units regardless of their taxonomic determination.

Microfacies data sheets were used to plot the occurrence of components (non-skeletal, skeletal, and terrigenous grain types), textural classification was done using Embry and Klovan's (1972) expanded version of Dunham's (1962) textural types. The relative abundance of particular grain types was established using the amount of each grain in thin section, according to the following criteria: more of 25 = Abundant; 16-25 = Frequent; 11-15 = Scarce; 6-10 = Rare; 1-5 = Trace. Some diagenetic observations such as isochemical features, including cement types, neomorphism and dissolution, were also obtained. All microfacies data were plotted on vertical sections displaying all the components, and an environmental and bathymetric interpretation of the succession was obtained (Fig. 4).

During the present investigation microfacies types (I-1 through VI-7) were defined within each lithic unit using the following criteria: 1) the type of texture, used to separate broad packages; 2) petrographic characteristics such as differences in micrite types; 3) presence of skeletal (fossils and fossil fragments); and 4) non-skeletal grains.

4.2. Description of Microfacies Types

Microfacies I-1: 0-337 m.- This interval is predominantly characterized by arkosic wackes with medium-sorted, angular to subangular quartz gains, calcareous grains are abundant locally. Subarkoses predominate in the upper part of this microfacies and are composed of medium to poorly sorted, angular to subangular grains. Microfacies I-1 was deposited in a Fan-Delta sedimentary environment.

Microfacies I-2: 337-376 m (Fig. 5-12).- This microfacies includes 39 meters of mudstone containing trace to rare quantities of skeletal grains including ostracod, echinoid, pelecypod, and algae fragments (Fig. 4). The matrix is homogeneous without any evidence of bioturbation.

Microfacies II-3: 376-468 m (Fig. 5-1, 5-2).- Mudstone/fossiliferous micrites to biomicrites. This interval is 92 meters thick of which the upper 72 meters are covered (see fig. 4). The remaining 18 meters are char-

acterized by fossiliferous micrites with abundant mollusk and echinoderm fragments. The diagenetic features present are coalescive neomorphism, solution seams, and dolomitization.

Microfacies II-4: 468-485 m (Figs. 5-17, 5-20).- Packstone/packed biomicrites and grainstone/biosparites. Only 17 meters of mainly packed biomicrites with biosparites at its base make up this microfacies. Most abundant skeletal allochems include: green algae, echinoderm fragments, ostracods, textularid foraminifera, and traces of rotalid foraminifera and gastropods (Fig. 4). The diagenetic features observed include "late cement" (most abundant) and "early cement" along with coalescive neomorphism, and some authigenic quartz.

Microfacies II-5: 485-510 m (Figs. 5-3, 5-4, 5-13).- Wackestone/biomicrites. Includes 25 meters of biomicrites with rare echinoderm and ostracod fragments, and traces of pelecypod and gastropod fragments. The diagenetic features include inversion, coalescive neomorphism, secondary porosity and solution seams (stylolites), dolomitization and dedolomitization, and authigenic quartz.

Microfacies II-6: 510-560 m.- Mudstone/shaley micrites. This microfacies consists of 50 meters of shales and shaley micrites in which the micrites lack completely of fauna or bioturbation. Coalescive neomorphism and secondary porosity are the only diagenetic features present.

Microfacies II-7: 560-580 m (Figs. 5-5, 5-6, 5-8).- Wackestone/biomicrites. Characterized by 15 meters of biomicrites and a 5 meter shale interval at the top. Nonskeletal allochems include intraclasts and pseudopellets. Skeletal grains include: abundant miliolids; frequent echinoderm fragments; scarce brachiopod, ostracod, and annelid fragments; and traces of pelecypod shells. Inversion, coalescive neomorphism and authigenic quartz are the diagenetic features present. Some terrigenous chert was also observed.

Microfacies II-8: 580-708 m (Figs. 5-7, 5-9, 5-11).- Mudstone/fossiliferous micrites to biomicrites and shaley micrites, dismicrites at base (sample AR32-50). This microfacies is 28 meters thick and is characterized by fossiliferous micrites and biomicrites with presence of intraclasts and fragments of brachiopods, echinoderms, ostracods, pelecypods and annelids; at the base, traces of gastropods, and abundant pelecypod fragments are present. "Late cement", inversion, coalescive neomorphism, and authigenic quartz were the diagenetic features observed.

Microfacies II-9: 708-740 m (Figs. 5-15, 5-16).- Grainstone/biopelsparites. This 32 meter interval is characterized by biosparites with abundant pellets, scarce ostracods, and traces of algae, brachiopod, and echinoderm fragments (Fig. 4). "Late cement", solution seams, dedolomitization, and authigenic quartz are the diagenetic features present.

Fig. 7.-Microfacies chracteristics and grain types found in Units III and IV: 1) Sample AR75-35. Biomicrite. Unit III-33-IV-33. Planktonic foraminifera *(Favusella* sp). 2) Sample AR77-25. Biomicrite. Unit III-33-IV-33. Planktonic echinoderm Saccocoma, ostracod fragments *(Microcalamoides diversus).* 3) Sample AR84-50. Biomicrite. Unit IV-35-V-35. Planktonic foraminifera *(Hedbergella delrioensis).* 4) Sample AR74-14. Biomicrite. Unit III-33-IV-33. Calpionellids *(Collomiella recta).* 5) Sample AR75-35. Biomicrite. Unit III-33-IV-33. Ostracod. 6) Sample AR68-25. Biomicrite. Unit III-33-IV-33. Planktonic foraminifera *(Hedbergella* sp). 7) Sample AR84-50. Biomicrite. Unit IV-35-V-35. Planktonic foraminifer *(Favusella washitensis),* calcisphaerulids *(Calcisphaerula inominata),* ostracod fragment (Microcalamoides?). 8) Sample AR69-50. Biomicrite. Unit III-33-IV-33. Benthic foraminifer *(Lenticulina* sp.) 9) Sample AR73-8. Biomicrite. Unit III-32. Planktonic foraminifer *(Hedbergella* sp). 10) Sample AR68-25. Biomicrite. Unit III-33-IV-33. Ostracod shell fragment *(Microcalamoides diversus),* calcisphaerulids *(Calcisphaerula inominata).* 11) Sample AR84-50. Biomicrite. Unit V-35-V-35. *Calcisphaerulids (Pithonella* sp., *Calcisphaerula inominata),* ostracod. 12) Sample AR68-25. Biomicrite. Unit III-33-IV-33. Planktonic foraminifer *(Favusella scitula).* 13) Sample AR74-14. Biomicrite. Unit III-33-IV-33. Calcisphaerulids *(Pithonella trejoi),* authigenic quartz. 14) Sample AR68-25. Biomicrite. Unit III-33-IV-33. Planktonic foraminifer (Favusella sp), calpionellids *(Colomiella mexicana).* 15) Sample AR80-15. Biomicrite. Unit IV-34. Planktonic foraminifer *(Ticinella* sp). 16) Sample AR68-25. Biomicrite. Unit III-33-IV-33. Benthic foraminifer (textularid). 17) Sample AR68-25. Biomicrite. Unit III-33-IV-33. Calpionellids *(Colomiella mexicana),* planktonic foraminifera *(Ticinella?)* and benthic foraminifer *(Lenticulina sp).* 8) Sample AR68-25. Biomicrite. Unit III-33-IV-33. Echinoderm fragment, calcisphaerulids, calpionellids *(Colomiella sp),* radiolarian. 19) Sample AR76-3. Calcareous shale. Unit III-32. Planktonic foraminifera *(Hedbergella* sp). Scale bar = 200 microns for all figures.

Fig. 7.-Tipos de granos y microfacies características identificados en las Unidades III y IV: 1) Muestra AR75-35. Biomicrita. Unidad III-33-IV-33. Foraminíferos planctónicos *(Favusella* sp). 2) Muestra AR77-25. Biomicrita. Unidad III-33-IV-33. Equinodermo planctónico: Saccocoma, fragmentos de ostrácodo *(Microcalamoides diversus).* 3) Muestra AR84-50. Biomicrita. Unidad IV-35-V-35. Foraminíferos planctónicos *(Hedbergella delrioensis).* 4) Muestra AR74-14. Biomicrita. Unidad III-33-IV-33. Calpionélido *(Collomiella recta).* 5) Muestra AR75-35. Biomicrita. Unidad III-33-IV-33. Ostrácodos. 6) Muestra AR68-25. Biomicrita. Unidad III-33-IV-33. Foraminíferos planctónicos *(Hedbergella* sp). 7) Muestra AR84-50. Biomicrita. Unidad IV-35-V-35. Foraminífero planctónico *(Favusella washitensis),* calciesferúlidos (Calcisphaerula inominata), fragmentos de ostrácodo (Microcalamoides?). 8) Muestra AR69-50. Biomicrita. Unidad III-33-IV-33. Foraminífero bentónico (Lenticulina sp). 9) Muestra AR73-8. Biomicrita. Unidad III-32. Foraminífero planctónico (Hedbergella sp). 10) Muestra AR68-25. Biomicrita. Unidad III-33-IV-33. Fragmento de ostrácodo *(Microcalamoides diversus),* calciesferúlidos *(Calcisphaerula inominata). 11)* Muestra AR84-50. Biomicrita. Unidad V-35-V-35. Calciesferúlidos *(Pithonella* sp., *Calcisphaerula inominata),* Ostrácodo. 12) Muestra AR68-25. Biomicrita. Unidad III-33-IV-33. Foraminífero planctónico *(Favusella scitula).* 13) Muestra AR74-14. Biomicrita. Unidad III-33-IV-33. Calciesferúlidos *(Pithonella trejoi),* cuarzo autígeno. 14) Muestra AR68-25. Biomicrita. Unidad III-33-IV-33. Foraminífero planctónico *(Favusella* sp), calpionélidos *(Colomiella mexicana).* 15) Muestra AR80-15. Biomicrita. Unidad IV-34. Foraminífero planctónico *(Ticinella* sp). 16) Muestra AR68-25. Biomicrita. Unidad III-33-IV-33. Foraminífero bentónico (textulárido). 17) Muestra AR68-25. Biomicrita. Unidad III-33-IV-33. calpionélidos *(Colomiella mexicana),* foraminíferos planctónicos *(¿Ticinella?)* y foraminífero bentónico (Lenticulina sp). 18) Muestra AR68-25. Biomicrita. Unidad III-33-IV-33. Fragmento de equinodermo, calciesferúlidos, calpionélidos *(Colomiella sp),* radiolarios. 19) Muestra AR76-3. Lutita calcárea. Unidad III-32. Foraminíferos planctónicos *(Hedbergella* sp). Escala = 200 micras para todas las figuras.

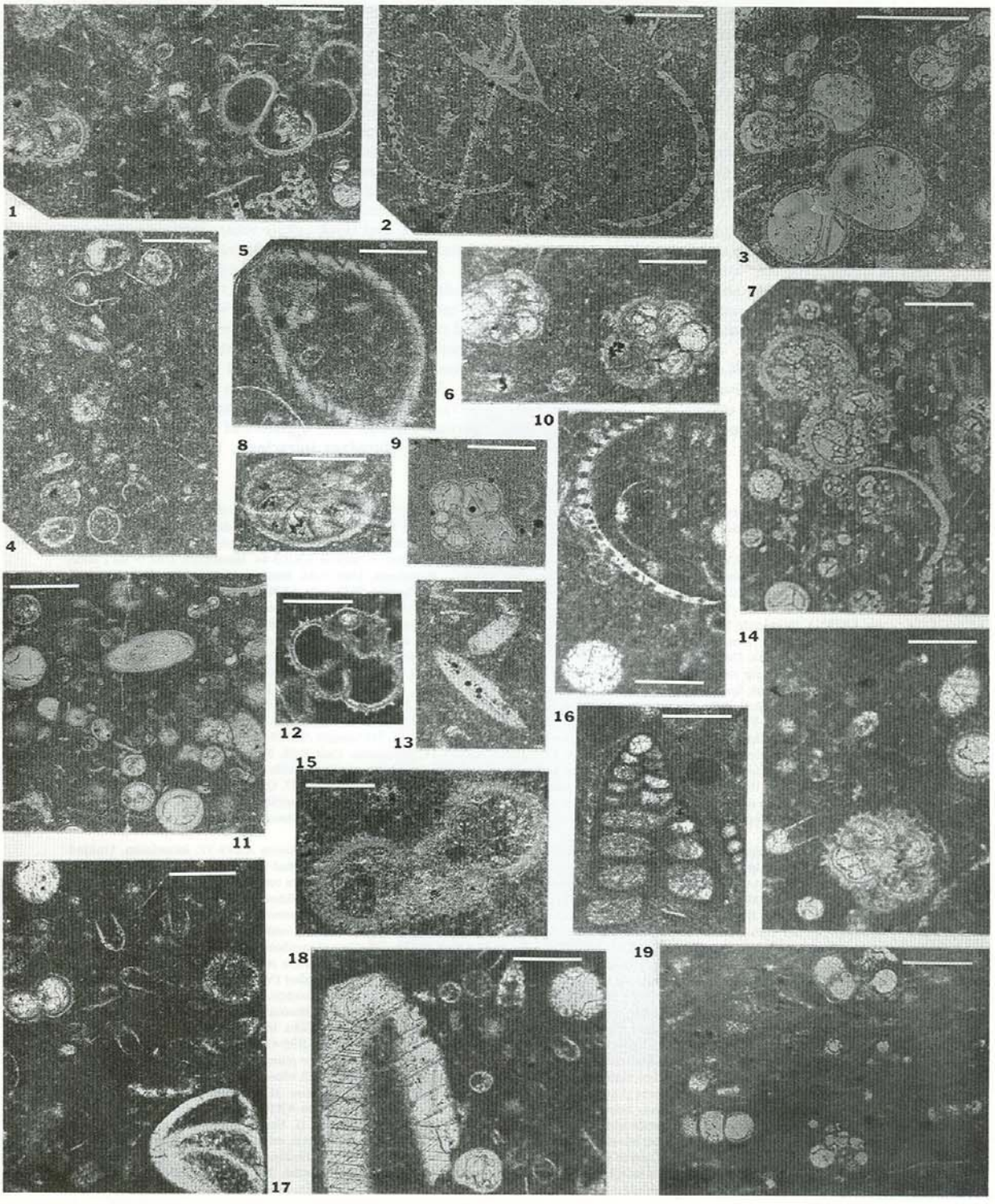
1
2
3
4
5
6
7
8
9
10
11
12
13
14
15
16
17
18
19

Microfacies II-10: 740-750 m.- Wackestone/dolomitic biomicrites. This interval is characterized by biomicrites with abundant pellets and frequent gastropod fragments. Coalescive neomorphism and very abundant dolomitization are the diagenetic features present.

Microfacies II-11: 750-788 m.- Mudstone/fossiliferous micrites to biomicrites. This microfacies is 38 meters thick of fossiliferous micrites and biomicrites with no allochems of any kind (Fig. 4). Only coalescive neomorphism, abundant rock fragments, and terrigenous quartz are present.

Microfacies II-12: 788-791 m (Figs. 5-18, 5-19; 5-20).- Grainstone/biointrasparites. Includes only 3 meters of biointrasparites with abundant intraclasts, miliolids, and gastropods, and frequent green algae. The diagenetic features observed are "early" and "late" cements and coalescive neomorphism. Terrigenous quartz grains are also common.

Microfacies II-13: 791-809 m.- Mudstone/micrites. This is an 18 meter interval of micrites with no allochems at all; only thick calcite veins, coalescive neomorphism, and terrigenous quartz grains were observed (Fig. 4).

Microfacies II-14: 809-831 m.- Wackestone/biomicrites. Includes 22 meters of biomicrites with abundant pseudopeloids, miliolids, and frequent echinoderm and mollusk fragments. Coalescive neomorphism and calcite veins are also present.

Microfacies II-15: 831-855 m (Figs. 6-1, 6-7, 6-14).- Grainstone/biosparite. Includes 24 meters of biosparites with abundant oolites, frequent miliolids, rare brachiopod fragments, scarce gastropods, and traces of ostracods. The diagenetic features observed are "early" and "late" cements, coalescive neomorphism, authigenic quartz, and thick calcite veins. Terrigenous quartz grains are also present in this interval.

Microfacies II-16: 855-873 m (Figs. 5-10, 6-6, 6-8).- Mudstone/fossiliferous micrites. Consists of 18 meters of mostly fossiliferous micrites with some intraclasts and traces of pelecypod and gastropod shells. The diagenetic features observed are "late cement", coalescive neomorphism, inversion, and dolomitization.

Microfacies II-17: 873-879 m (Figs. 6-4, 6-9, 6-11, 6-17).- Packstone/packed biointramicrites to biointrasparites. Includes only 6 meters of packed biointramicrites with abundant intraclasts, frequent ooids, rare

Fig. 8.-Microfacies chracteristics and grain types identified in Units IV, V, and VI: 1) Sample AR93-37. Biomicrite. Unit IV-35-V-35. Calcisphaerulids, planktonic foraminifera. 2) Sample AR89-50. Biomicrite. Unit IV-35-V-35. Calcisphaerulids, planktonic foraminifera.3) Sample AR105-35. Packed biomicrite. Unit V-36. Turbiditic texture, planktonic foraminifera. 4) Sample AR141-40. Biomicrite. Unit IV. Calpionellids *(Colomiella* spp), calcisphaerulids, planktonic foraminifera. 5) Sample AR103-44. Biomicrite. Unit V-36. Planktonic foraminifer *(Thalmanninella appenninica).* 6) Sample AR96-12. Biomicrite. Unit V-36. Benthic foraminifer *(Textularia).* 7) Sample AR103-44. Biomicrite. Unit V-36. Planktonic foraminifera *(Hedbergella* spp). 8) Sample AR88-43. Biomicrite. Unit IV-35-V-35. Planktonic foraminifer *(Ticinella floresae).* 9) Sample AR137-4. Biomicrite. Unit IV. Calcified radiolarian inside intraclast. 10) Sample AR137-4. Biomicrite. Unit IV. Planktonic foraminifer *(Thalmanninella ticinensis).* 11) Sample AR83-13. Biomicrite. Unit IV-35-V-35. Benthic foraminifer *(Lenticulina* sp.). 12) Sample AR85-13. Biomicrite. Unit IV-35-V-35. Calcified radiolarian. 13) Sample AR101-0. Biomicrite. Unit V-36. Calcified radiolaria, planktonic foraminifera. 14) Sample AR96-12. Biomicrite. Unit V-36. Planktonic foraminifer *(Thalmanninella ticinensis).* 15) Sample AR128-0. Biomicrite. Unit II. Reworked miliolid. 16) Sample AR85-13. Biomicrite. Unit V-36. Planktonic foraminifer *(Hedbergella planispira),* calcisphaerulids. 17) Sample AR88-43. Biomicrite. Unit IV-35-V-35. Calcisphaerulid *Bonetocardiella.* 18) Sample AR108-44. Biomicrite. Unit VI-37. Planktonic foraminifer?. 19) Sample AR108-44. Packed biomicrite. Unit VI-37. Planktonic foraminifera *(Hedbergella* spp), calcified radiolaria. 20) Sample AR101-0. Biomicrite. Unit V-36. Turbiditic texture, planktonic foraminifera *(Whiteinella* sp), calcified radiolaria. 21) Sample AR139-4. Biomicrite. Unit IV. Planktonic foraminifera, ostracods, echinoderm fragments. 22) Sample AR103-44. Biomicrite. Unit V-36. Planktonic foraminifera *(Whiteinella* spp). 23)Sample AR128-0. Biopelmicrite. Unit II. Unidentified planispiral foraminifer? inside intraclast. 24) Sample AR129-0. Biomicrite. Unit II. Pseudopeloids, miliolids?. 25) Sample AR109-30. Silty biomicrite. Unit VI-37. Quartz and feldspar silt. 26) Sample AR140-24. Biomicrite. Unit IV. Planktonic and benthic foraminifera, calpionellids. 27) Sample AR131-39. Biomicrite. Unit II. Fossil hash. 28) Sample AR110-43. Packed biomicrite. Unit VI-37. Mollusk fragments, calcisphaerulids. Scale bar = 200 microns for all figures.

Fig. 8.-Tipos de granos y microfacies características identificados en las Unidades IV, V, y VI: 1) Muestra AR93-37. Biomicrita. Unidad IV-35-V-35. Calciesferúlidos, foraminíferos planctónicos. 2) Muestra AR89-50. Biomicrita. Unidad IV-35-V-35. Calciesferúlidos, foraminíferos planctónicos. 3) Muestra AR105-35. Biomicrita empaquetada. Unidad V-36. Textura turbidítica, foraminíferos planctónicos. 4) Muestra AR141-40. Biomicrita. Unidad IV. calpionélidos *(Colomiella* spp), calcisferúlidos, foraminíferos planctónicos. 5) Muestra AR103-44. Biomicrita. Unidad V-36. Foraminífero planctónico *(Thalmanninella appenninica).* 6) Muestra AR96-12. Biomicrita. Unidad V-36. Foraminífero bentónico (Textularia). 7) Muestra AR103-44. Biomicrita. Unidad V-36. Foraminíferos planctónicos *(Hedbergella* spp). 8) Muestra AR88-43. Biomicrita. Unidad IV-35-V-35. Foraminífero planctónico *(Ticinella floresae).* 9) Muestra AR137-4. Biomicrita. Unidad IV. Radiolarios calcitizados, dentro de un intraclasto. 10) Muestra AR137-4. Biomicrita. Unidad IV. Foraminífero planctónico *(Thalmanninella ticinensis). 11)* Muestra AR83-13. Biomicrita. Unidad IV-35-V-35. Foraminífero bentónico *(Lenticulina* sp.). 12) Muestra AR85-13. Biomicrita. Unidad IV-35-V-35. Radiolarios calcitizados. 13) Muestra AR101-0. Biomicrita. Unidad V-36. Radiolarios calcitizados, foraminíferos planctónicos. 14) Muestra AR96-12. Biomicrita. Unidad V-36. Foraminífero planctónico *(Thalmanninella ticinensis).* 15) Muestra AR128-0. Biomicrita. Unidad II. Miliólido. 16) Muestra AR85-13. Biomicrita. Unidad V-36. Foraminífero planctónico *(Hedbergella planispira),* calciesferúlidos. 17) Muestra AR88-43. Biomicrita. Unidad IV-35-V-35. Calciesferúlido *Bonetocardiella.* 18) Muestra AR108-44. Biomicrita. Unidad VI-37. Foraminífero planctónico ?. 19) Muestra AR108-44. Biomicrita. Unidad VI-37. Foraminíferos planctónicos *(Hedbergella* spp), calcified radiolaria. 20) Muestra AR101-0. Biomicrita. Unidad V-36. Textura turbidítica, foraminíferos planctónicos (Whiteinella sp), radiolarios calcificados. 21) Muestra AR139-4. Biomicrita. Unidad IV. Foraminíferos planctónicos, ostrácodos, fragmentos de equinodermo. 22) Muestra AR103-44. Biomicrita. Unidad V-36. Foraminíferos planctónicos *(Whiteinella* spp). 23) Muestra AR128-0. Biopelmicrita. Unidad II. Foraminífero planiespiralado indeterminado, dentro de un intraclasto. 24) Muestra AR129-0. Biomicrita. Unidad II. Pseudopeloides, miliólidos?. 25) Muestra AR109-30. Biomicrita arcillosa. Unidad VI-37. Cuarzo y feldespato. 26) Muestra AR140-24. Biomicrita. Unidad IV. Foraminíferos planctónicos y bentónicos, calpionélidos. 27) Muestra AR131-39. Biomicrita. Unidad II. Fragmentos de fósiles. 28) Muestra AR110-43. Biomicrita. Unidad VI-37. Fragmentos de molusco (calciesferúlido). Escala = 200 micras para todas las figuras.

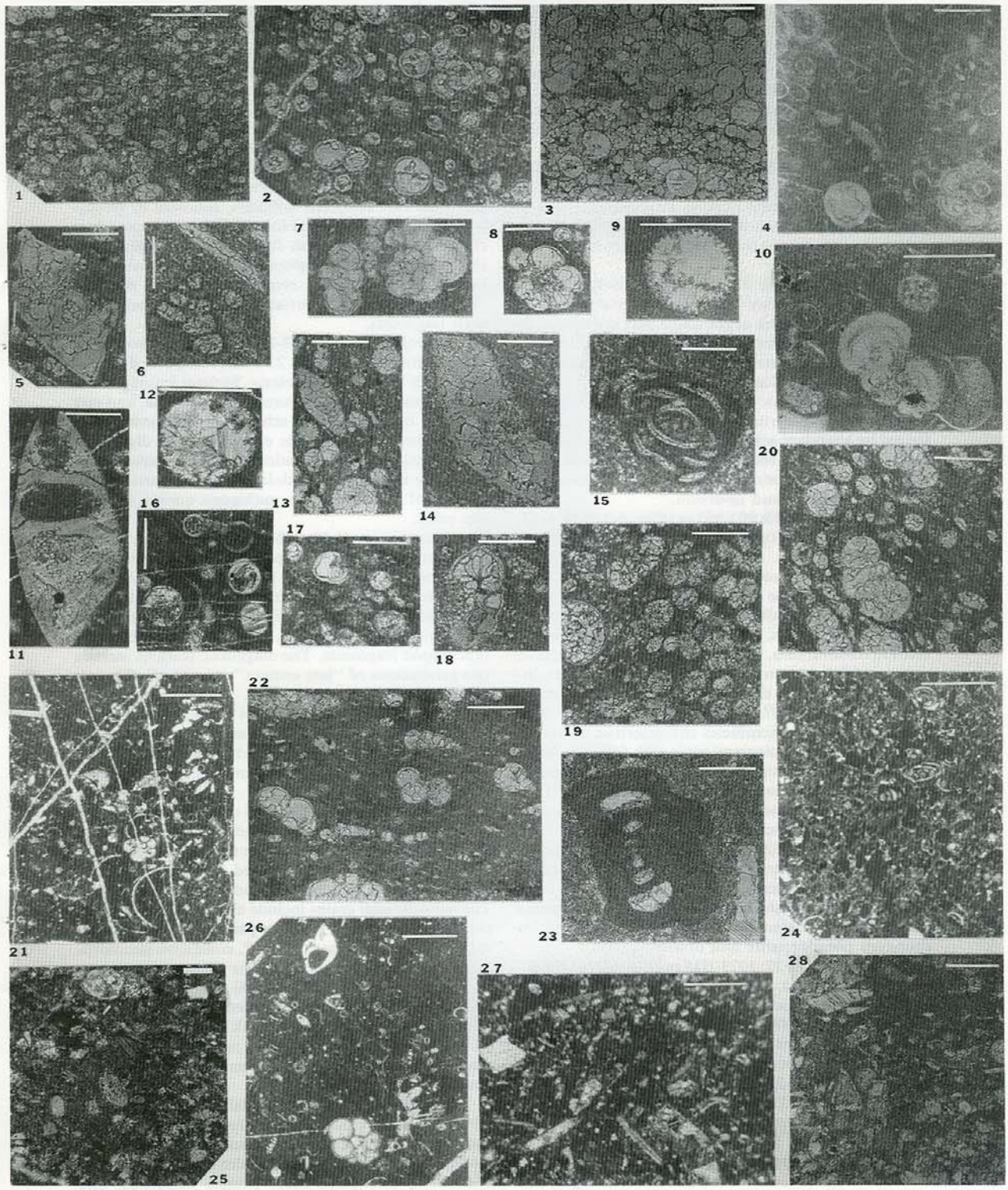
1
2
3
4
5
6
7
8
9
10
11
12
13
14
15
16
17
18
19
20
21
22
23
24
25
26
27
28

grapestones, abundant green algae, frequent miliolids and gastropods, and scarce brachiopod and pelecypod shell fragments. Micritic envelopes are abundant; often the allochems are leached and replaced by sparry calcite, remaining only the micritic envelopes. The diagenetic features include: "early"? and "late" cements, coalescive neomorphism, inversion, and authigenic quartz.

Microfacies II-18: 879-924 m.- Mudstone/fossiliferous micrites. This interval is 35 meters thick and is characterized by fossiliferous micrites with abundant pelecypod fragments and scarce echinoderm fragments. "Late cement" and inversion were the only diagenetic features observed.

Microfacies II-19: 924-962 m (Figs. 6-3, 6-5, 6-13, 6-15, 6-16).- Wackestone/biomicrites. 38 meter thick interval. The biomicrites of the lower part are characterized by having abundant ooids, frequent intraclasts and pseudopeloids, frequent miliolids, and rare rotalid benthic foraminifera. "Late cement", coalescive neomorphism, and authigenic quartz constitute the diagenesis present. The biomicrites of the upper part are characterized by abundant echinoderm and pelecypod (rudist) fragments, frequent textularid foraminifera, and scarce miliolids and ostracods. The diagenetic features present are "late cement" and inversion.

Microfacies II-20: 962-995 m (Figs. 6-2, 6-18, 6-23, 6-25).- Floatstone/biopelmicrudites. Includes 23 meters of biopelmicrudites. Non-skeletal grains present are abundant pseudopeloids, and frequent intraclasts. Skeletal allochems include abundant pelecypod (rudist) shell fragments, gastropods, green algae, textularid foraminifera, and miliolids, traces of ostracods and rotalid benthic foraminifera. The diagenetic features include: common "late cement", coalescive neomorphism, inversion, and partial silicification of shell fragments.

Microfacies II-21: 995-1019 m.- Wackestone/biointramicrites. The microfacies characteristic of this 24 meter interval are biointramicrites with frequent intraclast and abundant reworked miliolids and gastropods; most of them forming part of intraclasts. "Late cement" and coalescive neomorphism are the diagenetic features present.

Microfacies II-22: 1019-1073 m.- Mudstone/micrites and pseudosparites. Includes 54 meters of micrites almost bare of allochems except for a few intervals where abundant intraclasts and traces of mollusk fragments were observed. Extensive diagenesis is evidenced by abundant pseudosparite and dolomitization.

Microfacies II-23: 1073-1115 m (Fig. 6-22).- Floatstone/biomicrudites. Includes 42 meters of biomicrudites with abundant pelecypod rudist fragments and frequent echinoderm fragments. The diagenetic features include "late cement", inversion, and partial silicification of shell fragments.

Microfacies II-24: 1115-1148 m.- Mudstone-wackestone/biomicrites. This interval includes 33 meters of biomicrites with abundant reworked miliolids and echinoderm fragments, frequent orbitolinid foraminifera, and traces of pelecypod shells. "Late cement", coalescive neomorphism, and dolomitization were again the diagenetic features observed.

Microfacies II-25: 1148-1191 m.- Floatstone/biomicrudites. This microfacies interval is 43 meters thick of biomicrites lacking non-skeletal grains but contain mollusk (rudist ?), ostracod, and echinoderm fragments. Coalescive neomorphism and inversion are the diagenetic features present.

Microfacies II-26: 1191-1213 m (Figs. 6-10, 6-21).- Grainstone/biopelsparites. Includes 22 meters of biopelsparites with abundant pellets. Most abundant skeletal grains are reworked miliolids, followed by pelecypod fragments and rotalid foraminifera, and scarce brachiopod and echinoderm fragments; most allochems show heavy micritic envelopes. Diagenesis is evidenced by "early" and "late" cements, coalescive neomorphism, inversion, and partial silicification of pelecypod shell fragments.

Microfacies II-27: 1213-1240 m.- Packstone/packed biointramicrites. Includes 27 meters of packed biomicrites with abundant intraclasts. Skeletal grains include frequent miliolids, scarce rotalid foraminifera, and rare ostracod, brachiopod, and echinoderm fragments. Allochems show heavy micritic envelopes. The diagenesis present includes two generations of "late" cementation, coalescive neomorphism, dolomitization, partial silicification of shell fragments, authigenic quartz, and calcite veins.

Microfacies II-28: 1240-1263 m (Figs. 6-19).- Grainstone/biopelsparites-packed biopelmicrites. The grainstones of this 23 meter interval vary from biopelsparites to packed biopelmicrites with abundant pellets and miliolids; other allochems include frequent rotalid foraminifera and ostracods, and rare echinoderm and brachiopod fragments. The diagenetic features include two generations of "late cement", partial silicification of allochems, and calcite veins.

Microfacies II-29: 1263-1284 m.- Mudstone/micrites. Includes 21 meters of micrites with only scarce pelecypod shell fragments. Abundant sutured solution seams are present along with some coalescive neomorphism.

Microfacies II-30: 1284-1286 m.- Packstone/packed biointrapseudopelmicrites-packed biointrapseudopelsparites. This is a 2 meter interval of packestone that vary from packed micrites and packed sparites, but all having abundant pseudopeloids and frequent intraclasts. The main skeletal grains include abundant miliolid and pelecypod fragments, and rare gastropods and textularid foraminifera. "Late cement", coalescive neomorphism and inversion constitute the diagenesis present.

Microfacies II-31: 1286-1290 m.- Mudstone/fossiliferous micrites. Includes 4 meters of fossiliferous micrites with only abundant mollusk fragments. The diagenetic features include abundant pseudosparite and microsparite, sutured solution seams, and secondary porosity.

Microfacies III-32: 1290-1300 m (Figs. 6-12; 8-9, 8-19).- *Favusella* biomicrite and shale. This microfacies consists of 10 meters of planktonic foraminiferal-rich biomicrites and shale. Skeletal grains like planktonic foraminifera, calcisphaerulids, pelagic ostracods, and

echinoderm fragments are the predominate components. Terrigenous clay and quartz silt was observed throughout this interval.

Microfacies III-33-IV-33: 1300-1365 m (Figs. 8-1 to 8-6, 8-8, 8-10, 8-12 to 8-14, 8-16 to 8-18).- *Favusella-Colomiella* biomicrites. Includes 65 meters of predominantly planktonic skeletal grains including calpionellids, hedbergellids, favusellids, ostracods, and calcisphaerulids, along with textularid foraminifera. The rotalid foraminifer Lenticulina is also present at some intervals.

Microfacies IV-34: 1365-1418 m (Fig. 8-15).- *Ticinella-Hedbergella* biomicrites. Includes 53 meters of biomicrites with abundant planktonic foraminifera, pelagic ostracods, radiolaria, and abundant intraclasts in the middle of this interval. The foraminifer *Lenticulina* is present at the base.

Microfacies IV-35-V-35: 1418-1470 m (Figs. 8-3, 8-7, 8-11).- Calcisphaerulid biomicrites. This microfacies includes 52 meters of biomicrites rich in calcisphaerulids and planktonic foraminifera. Also present in various abundances are: pelagic ostracods, calcified radiolaria, benthic foraminifera, and pelecypod and gastropod fragments.

Microfacies V-36: 1470-1558 m (Figs. 8-3, 8-5 to 8-7, 8-13, 8-14, 8-20, 8-22).- Single-keeled hedbergellid biomicrites. Includes 107 meters of mudstones intercalated with shales. The mudstones are biomicrites with abundant radiolaria and keeled planktonic foraminifera. Minor abundances of other benthic foraminifera and mollusk fragments are also present.

Microfacies VI-37: 1558-1600 m (Figs. 8-18, 8-19, 8-25).- Radiolaria biomicrites to packed biomicrites. Includes 23 meters of biomicrites with occasional turbiditic texture, abundant radiolaria, and planktonic foraminifera. Terrigenous quartz and feldspar are abundant.

5. PALEOECOLOGICAL INTERPRETATION

In the present investigation the paleoecological interpretation of the Cretaceous succession studied was complicated by the fact that samples needed to be studied in thin-section of indurated carbonates. Consequently, the identification of paleontological components, bearing more ecological significance, could not be done beyond the Order or at best generic level. Skeletal (biological) grains are by far the most abundant components of the majority of the Cretaceous limestones analyzed where they are common to abundant. Fourteen skeletal grain types (biological components) were identified including: algae, annelids, brachiopods, calpionellids, calcisphaerulids, echinoderms, gastropods, miliolids, ostracods, pelecypods, planktonic foraminifera, radiolaria, rotalids (benthic calcareous), and textularids (Fig. 9). Grain composition as well as petrographic characteristic were used to interpret the paleoenvironment represented by each microfacies types.

The overall paleontological composition, as well as the predominance of carbonates, alternation of textural types related to high energy levels, and the lack of biological framestones (or barrier reefs) in the succession studied are indicative of a carbonate ramp in an open marine environment. The vertical distribution of the microfacies types was used to obtain a horizontal representation of an ideal depositional model which basically follows Walther's law of facies (Middleton, 1973). The Campeche ramp in the Gulf of Mexico is considered as a present-day analog of the environmental model represented by the Cretaceous succession studied.

Foraminifera were used as depth indicators, water depths were based on the generic determinations of foraminfera according to the work by Estavillo (1976) in the Campeche ramp, Culver (1988) in the northwestern Gulf of Mexico, and Longoria (1975) on the Comanchean Series in northeastern Mexico. Following the results by Estavillo (1976) the planktonic/benthonic ratio of foraminifera present in the thin-section was also used as a paleobathymetric index for the carbonate ramp. The relative abundance of non-keeled and keeled planktonic foraminifera was interpreted following the results by Longoria (1975). In spite of our use of multiple criteria to obtain paleoenvironmental interpretations of the succession studied, we are aware of the limitations in obtaining paleobathymetic determinations based on microfossils. However, as stated by Luterbacher (1984, p. 396): *"En general, las interpretaciones paleobatimétricas exigen una actitud pragmática y un razonamiento basado en varios métodos, es preciso seguir varias vías de argumentación y de confrontar continuamente las conclusiones con las basadas en otras disciplinas hasta poder llegar a un resultado coherente y geológicamente razonable."* Furthermore, we anticipate that adequate paleoenvironmental evaluations are drawn which are coherent with the depositional history of the Mesozoic of northeastern Mexico.

5.1. Inner Ramp

Microfacies.- The Inner Ramp is represented by the following microfacies types: I-2, II-3, II-4, II-5, II-6,II-8, II-9, II-10, II-11, II-13, II-16, II-18, II-22, II-23, II-25, II-29.

Water depth.- Shallow open marine (inner zone) to 50 m. Including the transitional zone between 0 and 20 m in which two major sedimentary environments can be recognized: 1) supratidal: highest incursion of marine waters (microfacies II-3, II-5, II-11, II-13), and 2) intertidal: zone of constant wave action, between low and high tides (Microfacies II-6, II-16). Locally high energy banks made of grainstones are formed (Microfacies II-4, II-9).

Paleontological components.- The following groupings were distinguished: 1) extremely rare to lacking of biological components (supratidal), 2) typically made of only one biological component (intertidal), 3) two biological components (open inner ramp below the influence of tides) and lacking planktonic foraminifera or extremely rare.

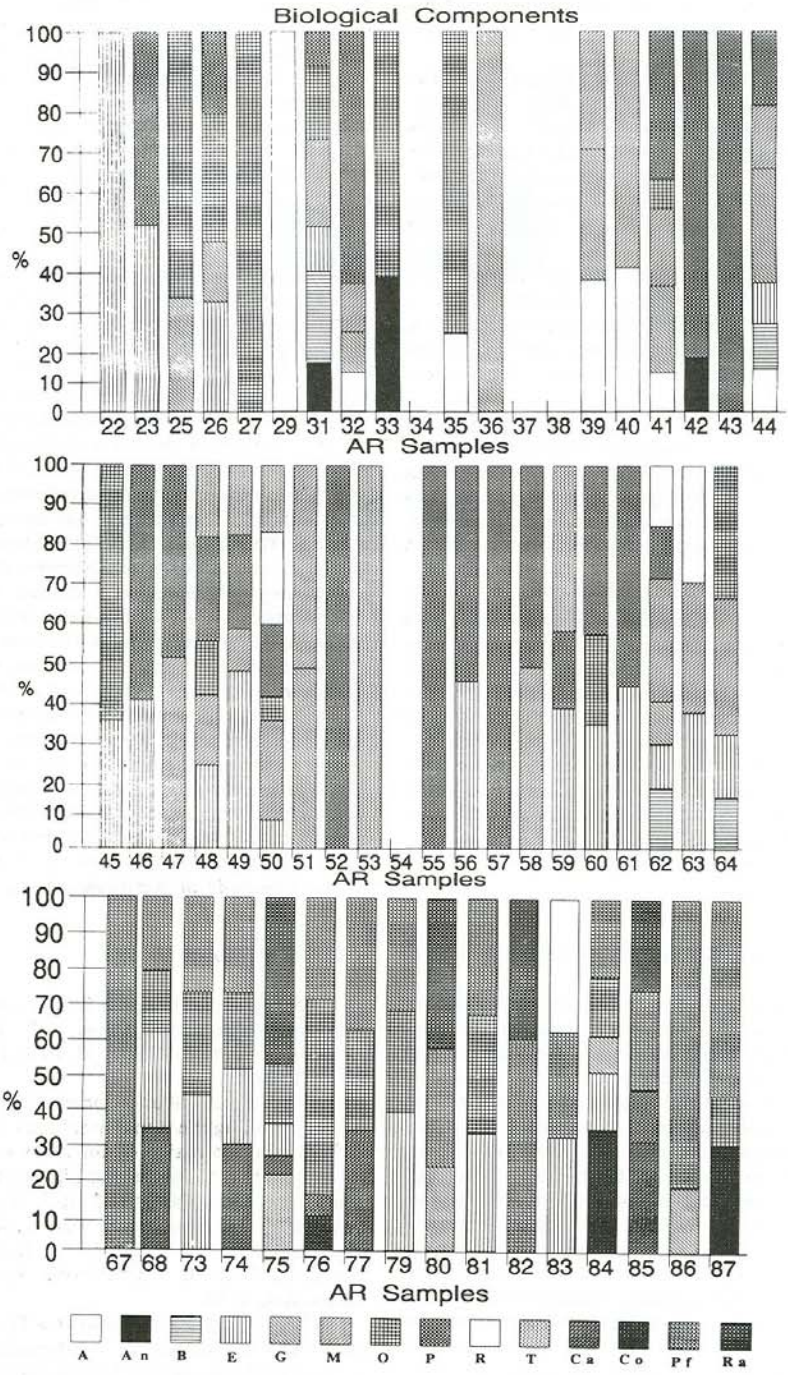

Fig. 9.- Bar diagrams showing percentages of skeletal grain types in individual samples of the El Chorro section. Both the number of components and the quantitative relation of each grain in the samples were considered of paleoecological siginificance.

Fig. 9.- Diagramas en barra que muestran los porcentajes de granos esqueléticos en cada una de las muestras de la sección El Chorro. Tanto el número de componentes como la cantidad de cada tipo de grano en las muestras fueron considerados de significado paleoecológico.

5.2. Middle Ramp

Microfacies.- The Middle Ramp environments are represented by the following microfacies types: II-7, II-12, II-14, II-15, II-17, II-19, II-21, II-24, II-27, II-28, II-30.

Water depth.- Middle zone (51 m to 100 m).

Paleontological components.- Abundant to common miliolids (quinqueloculinids and nummoluculinids), rotalids. Planktonic foraminifera are rare, but if present less than 10 percent. Diverse amounts of mollusk, echinoderms, calcareous algae. Locally rudists (requienids and caprinids) become abundant developing shoals and carbonate mounds (Microfacies II-12, II-15,). Lagoonal environments are also developed at some intervals (Microfacies II-7, II-4, II-21).

5.3. Outer Ramp

Microfacies.- The outer ramp is only represented in microfacies III-32, III-33, and IV-33.

Water depth.- Deeper water (101 to 200 m).

Paleontological components.- Abundant (40 to 50 percent) non-keeled planktonic foraminifera (hedbergellids, favusellids), common mollusk, coral, and echinoderm debris. Ostracods (Microcalamoides) are frequent.

5.4. Slope/Basin Margin

Microfacies.- IV-33, IV-35, V-35.

Water depth.- Upper bathyal zone (below 200 m).

Paleontological components.- Abundant planktonic foraminifera, colomiellids, calcisphaerulids, and mollusk, and echinoid debris. Benthic foraminifera are locally common consisting of lenticulinids.

5.5. Basin

Microfacies.- Basinal facies are represented by microfacies types VI-36, and V-37.

Water depth.- Middle bathyal zone (below 500 m).

Paleontological components.- Abundant (more that 75 percent) keeled planktonic foraminifera and common radiolaria. Very rare fragmental grains such as mollusks and echinoids. Pelagic echinoids (saccocomids) are commonly found.

6. DEPOSITIONAL ENVIRONMENTS

The stratigraphic succession exposed at La Nieve Anticline can be interpreted in terms of its sedimentary systems and depositional environments as follows:

6.1. Fan-delta sedimentation

Terrigenous sediments of the lower part of the section characterize the sedimentation in a basin adjacent to an active strike-slip fault regime in which fluviodeltaic and fan-delta sedimentation was generated as a result of fault reactivation (Fig. 10). As a result, thick piles of terrigenous sediments were deposited in the fault-bounded basin margins, whose lateral extent was very limited. Rapid sedimentation associated to fault activity accounts for the re-working of Lower Cretaceous faunas. The initiation of this fault activity is unknown, but it is clear that ended in the Bedoulian (Biozone K-7). At this time a more stable carbonate system developed (Fig. 10) and lasted until the Vraconian (Biozone K-17).

6.2. Shallow water carbonates

The contact between Unit I and Unit II marks the beginning of a predominantly carbonate sedimentary environment. This change in sedimentation is attributed to a time of tectonic stability whereby thermotectonic subsidence was taking place (Fig. 11). Shallow water carbonates of the Cupido Limestone were deposited on a wide ramp with open communication to marine conditions which developed on top of the terrigenous succession (Fig. 10A). No reef barrier was formed at the site of, or nearby La Nieve Anticline area. Microfacies types and lithic units are distributed as follows:

Depositional environment	*Lithic Unit*	*Microfacies*
Inner Ramp	II	2-6, 8-11, 13
Middle Ramp	II	7, 14-16, 19-21
Outer Ramp	II	12, 17-18, 23-31

The geohistory curve of Figure 11 shows that shallow-water carbonate deposition lasted for about 4.5 m.y. The great thickness (914 meters) of Unit II is explained assuming a stand of sea level coupled with progradation and gradual subsidence, implying accumulation rates of 20.31 cm/1000 year and a subsidence rate of 19.64 cm/1000 year in 4.5 m.y. Changes in sedimentary environments, from supratidal to outer ramp, through Unit II represent progradation-aggradational cycles.

6.3. Deep water carbonates

The contact between Unit II and Unit III (Cupido-La Peña? contact) reflects abrupt environmental changes, from outer ramp to slope/basin, which are explained via a major transgressive event with the resulting drowning of the carbonate ramp. Microfacies types and lithic units are distributed as follows:

Depositional environment	*Lithic Unit*	*Microfacies*
Slope	III	33
	IV	35
	V	35

The thermotectonic subsidence that took place during deposition of Unit III is likely to be related to active sea-floor spreading in the Atlantic during Aptian. The La Peña transgressive event likely reflects the timing of magnetic anomaly 0 in the Atlantic and the opening of the south Atlantic. Planktonic foraminiferal faunas present in unit 3 are remarkably similar to those described from Madagascar (Sigal, 1966; Longoria, 1974).

Unit III-Unit IV contact reflects the continuation of a transgressive event expressed in local fluctuations and an environmental change in the area from ramp-margin to slope. Unit IV-Unit V contact (Tamaulipas?-Cuesta del Cura contact) marks a change in bathymetry as the later unit represents sedimentation in bathyal depths.

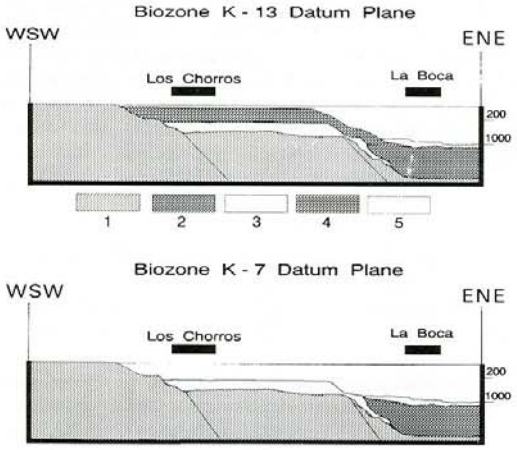

Fig. 10.-Aptian evolution of depositional environments prevailing during the deposition of Units I and II represented in Cañon El Chorro section, and their genetic relation to La Boca Canyon succession: A) Lower Aptian (Biozone K-7). B) Upper Aptian (Biozone K-13). Legend: 1.-Continental basement. 2.-Deep water carbonates of San Angel Limestone. 3.-Fan-delta siliciclastics of Unit I. 4.-Shallow water carbonates of the Cupido Limestone. 5.-La Peña Formation.

Fig. 10.-Evolución en el Aptiense de los ambientes deposicionales prevalecientes durante el depósito de las Unidades I y II representadas en la sección del Cañon El Chorro, asi como sus relación genéticas con los sedimentos de aguas profundas de la sucesión del Cañon de La Boca. A) Aptiense Inferior (Biozona K-7). B) Aptiense Superior (Biozona K-13). Leyenda: 1.-Basamento continental. 2.-Carbonatos de aguas profundas de la Caliza San Angel. 3.-Siliciclásticos fluviodeltaicos de la Unidad I. 4.-Carbonatos de aguas someras de la Caliza Cupido. 5.-Formación La Peña.

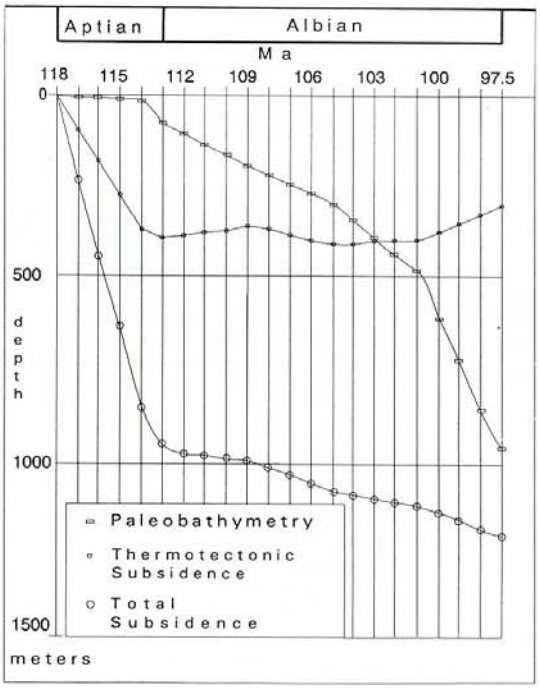

Fig 11.-Geohistory curve showing the Aptian-Albian subsidence history of the La Nieve succession. Its interpretation is given in the text.

Fig. 11.-Curva de la historia geológica en la que se muestra la subsidencia durante el Aptiense-Albiense de la sucesión de la Sierra La Nieve. La interpretaión se dá en el texto.

6.4. Flysch deposition

The first occurrence of shale, argillaceous limestone, and bentonite of the Agua Nueva defines the beginning of pelitic flysch, whose deposition indicates tectonic activity in the region. Tectonic activity in the region is also evidenced by the thermotectonic subsidence curve of Fig. 22.

7. CONCLUSIONS

Both limbs of La Nieve Anticline contain lithic units with equal thickness which permits geometric reconstructions of the anticlinal fold (Fig. 2).

The units identified in the field can be lithocorrelated as follows:

Lithic Unit:	*Present Work*	*Previous Workers*
Unit VI	Agua Nueva	Hendidura
Unit V	Cuesta del Cura	Cuesta del Cura
Unit IV	Tamaulipas?	Aurora
Unit III	La Peña?	La Peña
Unit II	Cupido	Cupido
Unit I	?	Taraises-Casita

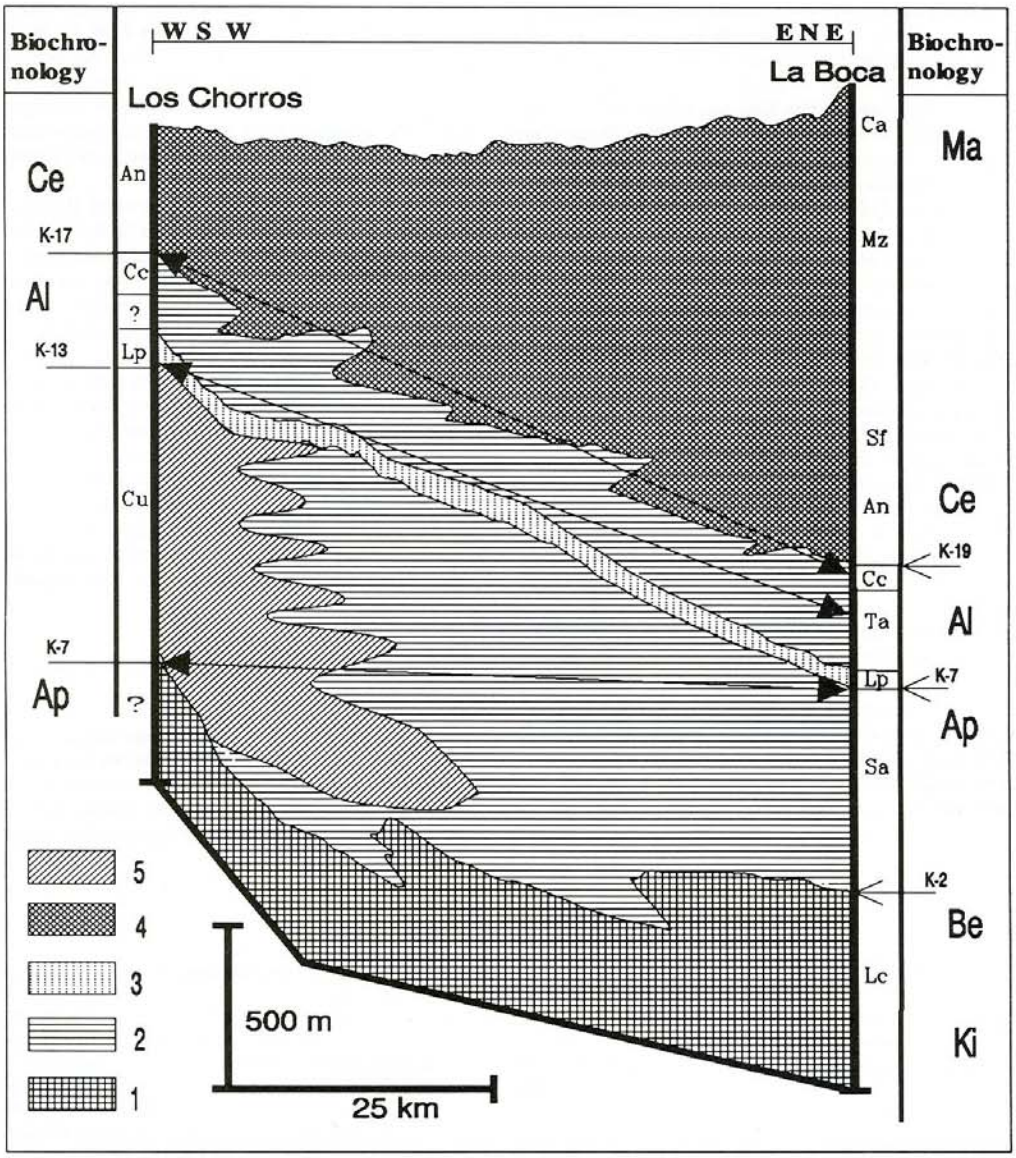

Fig. 12.-Regional correlation of physical stratigraphic events across northeast Mexico. Events recognized in Cañon El Chorro section are correlated with similar event as observed at La Boca Canyon and Sierra de Parras succession. La Boca Canyon section after Longoria and Davila (1978), Sierra de Parras after Imlay (1936, 1937). Legend: An.-Agua Nueva Formation. Au.-Aurora Limestone. Ca.-Caracol Formation. Cc.-Cuesta del Cura Formation. Ce.-El Cercado Formation. Cu.-Cupido Limestone. In.-Indidura Formation. Lc.-La Caja Formation. LCa.-La Casita Formation. Lg.-La Gloria. Lp.-La Peña Formation. Mz.-Mendez Shale. Pa.-Parras Shale. Sa.-San Angel. Sf.-San Felipe. Ta.-Tamaulipas Limestone. Biochronologic data: Ki.-Kimmeridgian. Be.-Berriasian. Ap.-Aptian. Al.-Albian. Ce.-Cenomanian. Ma.-Maastrichtian. K2, K7, K13, K-17, K19 biozones in Longoria's (1984c) biochronologic scheme.

Fig. 12.-Correlación regional de eventos físicos estratigráficos en el noreste de México. Los eventos reconocidos la sección del Cañon El Chorro son correlacionados con eventos similares que se observan en el Cañon de La Boca y la sucesión de la Sierra de Parras. La sección del Cañon de La Boca Canyon según Longoria and Davila (1978), la de la Sierra de Parras según Imlay (1936, 1937). Leyenda: An.-Formación Agua Nueva. Au.-Caliza Aurora. Ca.-Formación Caracol. Cc.-Formación Cuesta del Cura. Ce.-Formación El Cercado. Cu.-Caliza Cupido. In.-Formación Indidura. Lc.-Formación La Caja. LCa.-Formación La Casita. Lg.-Formación La Gloria. Lp.-Formación La Peña. Mz.-Lutita Mendez. Pa.-Lutita Parras. Sa.-Caliza San Angel. Sf.-Formación San Felipe. Ta.-Caliza Tamaulipas. Datos biocronológicos: Ki.-Kimmeridgiense. Be.-Berriasiense. Ap.-Aptiense. Al.-Albiense. Ce.-Cenomaniense. Ma.-Maastrichtiense. K2, K7, K13, K-17, K19 biozonas del esquema biocronológico de Longoria (1984c).

Physical stratigraphic events in the Cretaceous (Fig. 12) include: *Event 1*, identified by the deposition of a continuous carbonate succession (Cupido and San Angel Formations). *Event 2*, drowning of the carbonate platforms, expressed in the first appearance of terrigenous shales of La Peña and Unit III, at la Boca Canyon and Los Chorros Canyon, respectively. *Event 3*, beginning of the pelitic flysch sedimentation (Agua Nueva Formation). *Event 4*, beginning of the arenaceous flysch sedimentation. This event was not documented at Los Chorros Canyon but is well observed elsewhere in northern Mexico such as in the Parras region of Coahuila state. The correlation of these events across northeastern Mexico; to the ENE of Los Chorro into La Boca Canyon, and to the WSW of Los Chorros into Sierra de Parras, is shown in Fig. 12.

As stated above, no fossils were observed in the terrigenous lower part of the succession during the course of the present investigation. However, the presence of *Parhabdolitus asper* (Stradner) in the upper part of Unit I, as reported by Barrier (1977, p. 295), bracketed by the presence in Unit III of Upper Aptian planktonic foraminifera of Biozone K-13 indicates that carbonate deposition started in the Bedoulian (Lower Aptian).

The abundance of planktonic foraminifera (hedbergellids, favusellids, and ticinellids) in Unit III permitted to assign its base to Biozone K-13 (uppermost Aptian). Consequently, the chronostratigraphic position of La Peña lithofacies in northern Mexico varies from lower Aptian (Biozone K-7) in La Boca Canyon to upper Aptian (Biozone K-13) in Los Chorros section. The use of La Peña as a Gargasian "time horizon" as implied by previous authors (Smith, 1981) should be avoided. Our biochronologic studies showed that La Peña is a time transgressive unit from ESE to WNW.

Similarly, the debut of the flysch deposition (Agua Nueva Formation) in the region corresponds to a diachronous event; however, this event is younger at Los Chorros, Biozone K-17 (Vraconian/Cenomanian) and older at La Boca Canyon, Biozone K-19 (Upper Cenomanian) (Figure 12).

The difference in polarity between the terrigenous pulses of Event 2 and Event 3, that is, the fact that Event 2 is older to the ENE whereas the contrary occurs with Event 3 is difficult to interpret due to the lack or widely distributed sections. Nonetheless, one possible explanation may be that both successions developed in separate basins since the Albian.

The application of microfacies analysis to the study of carbonate succession, as exemplified in this study, offers the potential of utilizing both petrographic and micropaleontological data obtained in thin-sections of indurated lithologies to obtain chronostratigraphic, paleoecological, and sedimentological interpretations which will be valuable to geologists as an alternative in interpreting sedimentary environments, as well as an alternative characterization of lithostratigraphic units.

ACKNOWLEDGMENTS

Field work for this project was supported by a Research Grant from the Jet propulsion Laboratory. The authors would like to thank the Programs in Geosciences of the University of Texas at Dallas for providing the laboratory facilities to complete this research.

REFERENCES

Barrier,J. (1977): Study of the coccoliths and *Nannoconus* from the Taraises-Cupido shelf margin, northern Mexico. In: Bebout, D.G. and Loucks, R.G., (Eds.): *Cretaceous carbonates of Texas and Mexico.* University of Texas at Austin, Bureau of Economic Geology Report of Investigation no. 89: 295-298.

Bonet,F. (1956): *Zonificación microfaunística de las calizas del Este de México.* XX International Geological Congress, Mexico City, Monograph 115 p.

Bose,E. (1923): Vestiges of an ancient continent in northeast Mexico. *Amer. Jour. Sci.,* 6: 127-136, 196-214 & 310-337.

Brown,J.S. (1943): Suggested use of the word microfacies: *Econ. Geol.,* 38: 325.

Burckhardt,C. (1930): Etude synthétique sur le Mesozoique Mexican. *Societé Paleontol. Suisse,* Memoire 49-50, 280 p.

Carozzi,A.V. (1989): *Carbonate rock depositional models: A microfacies approach.* Prentice Hall, Advanced Reference Series, Physical and Life Sciences 604 p.

Conklin,J. and Moore,C. (1977): Paleoenvironmental analysis of the Lower Cretaceous Cupido Formation. In: Bebout, D.G. and Loucks, R.G., (Eds.): *Cretaceous carbonates of Texas and Mexico,* University of Texas at Austin, Bureau of Economic Geology Report of Investigation no. 89: 302-323.

Cserna,Z. (1956): *Tectónica de la Sierra Madre Oriental de México entre Torreón y Monterrey.* XX International Geological Congress, Mexico City, Monograph 87 p.

Culver,S.J. (1988): New foraminiferal depth zonation of the northwestern Gulf of Mexico. *Palaios,* 3: 69-85.

Cuvillier,J. (1961): Etude et utilisation rationalle de microfacies. *Revue Micropal.,* 4: 3-6.

Dunham,R.J. (1962): Classification of carbonate rocks according to depositional texture. In: W.E Ham (Ed.): *Classification of carbonate rocks.* Amer. Assoc. Petrol. Geol. Memoir 1: 108-121.

Ekdale,A.A., Ekdale,S.F. and Wilson,J.L. (1976): Numerical analysis of carbonate microfacies in the Cupido Limestone (Neocomian-Aptian), Coahuila, Mexico. *Jour. Sed. Petrol.,* 46: 362-368.

Embry,A.F. and Klovan,E.J. (1972): Absolute water depth limits of late Devonian paleoecological zones. *Geol. Rudsch.,* 61/2.

Estavillo,F.(1976): Estudio micropaleontológico de algunos sedimentos del Reciente del Golfo de México. *Sociedad Geológica Mexicana Boletín,* 37: 32-48.

Flügel,E. (1982): *Microfacies analysis of limestones.* Berlin,

Heidelberg, Springer-Verlag, 633 p.

Fortunato,K.S. (1982): *Depositional Framework of the La Casita Formation (Upper Jurassic-Lower Cretaceous), near Saltillo, Coahuila, Mexico.* Unpublished M.S. Thesis, The University of New Orleans, 278 p.

Fortunato,K.S. and Ward,W.C. (1982): Upper Jurassic-Lower Cretaceous fan-delta complex, La Casita Formation of the Saltillo area, Coahuila, Mexico. *Gulf Coast Association of Geological Societies Transactions,* 32: 473-482.

Guzman,A.E. (1974): Diagénesis de la Caliza Cupido del Cretácico Inferior. Coahuila, México. *Instituto Mexicano del Petroleo Revista,* 6: 20-40.

Humphrey,W.E. (1949): Geology of Sierra de Los Muertos area, Mexico (with descriptions of Aptian cephalopods from the La Peña Formation). *Geol. Soc. Amer. Bull.,* 60: 89-176.

Imlay,R.W. (1936): Evolution of the Coahuila Peninsula, Mexico, Part IV. Geology of the western part of the Sierra de Parras. *Geol. Soc. Amer. Bull.,* 47: 1091-1152.

Imlay,R.W. (1937): Geology of the middle part of the Sierra de Parras, Coahuila, Mexico. *Geol. Soc. Amer. Bull.,* 48: 587-630.

Imlay,R.W. (1938): Studies of the Mexican Geosyncline. *Geol. Soc. Amer. Bull.,* 49: 1651-1694.

Kliest,R., Hall,S.A., and Evans,I. (1984): A paleomagnetic study of the Lower Cretaceous Cupido Limestone, northeast Mexico: Evidence for local rotation within the Sierra Madre Oriental. *Geol. Soc. Amer. Bull.,* 95: 55-60.

Longoria,J.F. (1968): Estudio en sección delgada de algunas especies del Género Globotruncana (Cushman) del Este-Central de México. *Asociación Mexicana de Geólogos Petroleros Boletín, 20: 41-117.*

Longoria,J.F. (1974): Stratigraphic, morphologic, and taxonomic studies of Aptian planktonic foraminifera. *Rev. Esp. Micropal.,* número especial diciembre 1974, 107 p.

Longoria,J.F. (1975): Estratigrafía de la Serie Comancheana del Noreste de México. *Sociedad Geológica Mexicana,* XXXVI: 31-59.

Longoria,J.F. (1977): Bioestratigrafía del Cretácico Superior basada en foraminíferos planctónicos. *Univ. Nal. Autón. México, Inst. Geología, Revista,* 1: 10-22.

Longoria,J.F. (1984a): Stratigraphic Studies in the Jurassic of Northeastern Mexico: Evidence for the origin of the Sabinas Gulf. *Soc. Econ. Paleont. Mineral., Gulf Coast Section, Annual Res. Conf. Proceedings:* 171-193.

Longoria,J.F. (1984b): Mesozoic tectostratigraphic domains in east-central Mexico. In: G.E.G. Westerman (Ed.), Jurassic-Cretaceous biochronology and paleogeography of North America. *Geol. Assoc. Canada,* Sp.Paper 27: 65-76.

Longoria,J.F. (1984c): Cretaceous biochronology from the Gulf of Mexico region based on planktonic microfossils. *Micropaleontology,* 30: 225-242.

Longoria,J.F. (1985): Tectonic transpression in the Sierra Madre Oriental, northeastern Mexico: an alternative model. *Geology,* 13: 453-456.

Longoria,J.F. (1988): Late Triassic-Jurassic paleogeography and origin of Gulf of Mexico Basin: Discussion. *Amer. Assoc. Petrol. Geol. Bull.,* 72: 1411-1418.

Longoria,J.F. and Dávila,V.M. (1978): Estratigrafía y microfacies del Cerro de La Silla, SE de Monterrey. *Universidad de Sonora, Departamento de Geología Boletín,* 2: 65-95.

Longoria,J.F., and Gamper,M.A. (1974): Albian planktonic foraminifera from the Sabinas Basin of northern Mexico. *Actes 6o. Col. Africain Micropal.* Túnez, 28: 39-71.

Luterbacher,H.P. (1984): Paleobatimeria basada en microfósiles-Problemas y posibilidades. In: A. Obrador (ed.), *Libro Homenaje a L. Sanchez de la Torre,* Publ. Geol. Barcelona, 391-397.

Manivit,H. (1971): *Nannofossiles calcaires du Crétacé français (Aptien-Maestrichtien). Essai de biozonation appuyée sur les stratotypes.* Theses Univ. Paris, 187 p.

Middleton, G.V. (1973): Johannes Walther's Law of the correlation of facies. *Geol. Soc. Amer. Bull.,* 84: 979-988.

Muir,J.M. (1936): *Geology of the Tampico region, Mexico.* Amer. Assoc. Petrol. Geol., Tulsa, Okla., 200 p.

Muslow,M.H. (1983): *Petrography of the Lower Cretaceous Cupido Formation in San Lorenzo Canyon, Saltillo, Coahuila, Mexico.* MS thesis, The University of Southern Louisiana, 69 p.

Pessagno,E.A.Jr. (1967): Upper Cretaceous planktonic foraminifera from the western Gulf Coastal Plain. *Palaeontographica Americana,* 5: 245-444.

Ramírez del Pozo,J. (1971): Bioestratigrafía y microfacies del Jurásico y Cretácico del Norte de España (Región Cantábrica). *Mem. Inst. Geol. Min. España,* 3 tomos, 358 p.

Salisbury,B.L. (1982): *Petrology of the La Casita Formation in Chorro and Cortinas canyons, northeastern Mexico.* M.S. Thesis, The University of New Orleans, 173 p.

Sigal,J. (1966): Contribution a une monographie des Rosaliines. 1. Le genre Ticinella Reichel souche des Rotalipores. *Ecl. Geol. Helv.,* 59: 185-217.

Smith,C.I. (1981): Review of the geologic setting, stratigraphy, and facies distribution of the Lower Cretaceous in northern Mexico. In: S.M.Katz and C.I.Smith (Eds.), *Lower Cretaceous stratigraphy and structure, northern Mexico. West Texas Geological Society, Field trip Guidebook,* November 11-16, 1981, Publ. No. 81-74: 78-84.

Thierstein,H.P. (1973): Lower Cretaceous calcareous nannoplankton biostratigraphy, *bhandlungen der Geologischen Bundesanstalt* 29: 1-52.

Wilson,J.L. (1975): *Carbonate facies in geologic history* Springer-Verlag, Heidelberg, 471 p.

Wilson,J.L. (1981): Lower Cretaceous stratigraphy in the Monterrey-Saltillo area. In: S.M. Katz, and C.I. Smith (Ed.), *Lower Cretaceous stratigraphy and structure, northern Mexico.* West Texas Geological Society, Field trip Guidebook, November 11-16, 1981, Publ. No. 81-74.

Wilson,J.L. and Pialli,G. (1977): A Lower Cretaceous shelf-margin in northern Mexico. In: D.G. Bebout, and R.G. Loucks (Eds.), *Cretaceous carbonates of Texas and Mexico.* University of Texas at Austin, Bureau of Economic Geology Report of Investigation, 89: 286-294.

Recibido 17 de abril de 1990
Aceptado 2 de noviembre de 1990